Remote Sensing of Environment 334 (2026) 115199

Contents lists available at ScienceDirect

Remote Sensing of Environment

journal homepage: www.elsevier.com/locate/rse

# Sentinel-1 imagery for wide-scale quantitative landslide vulnerability assessment of buildings☆

Francesco Poggi [a,b], Francesco Caleca [a], Olga Nardini [a], Francesco Barbadori [a], Matteo Del Soldato [a], Claudio De Luca [b], Francesco Casu [b], Manuela Bonano [b], Riccardo Lanari [b], Veronica Tofani [a], Federico Raspini [a,*]

[a] Earth Sciences Department, University of Florence, Via La Pira 4, Firenze, Italy
[b] IREA – CNR, Istituto per il Rilevamento Elettromagnetico dell'Ambiente, Via Diocleziano 328, Napoli, Italy

ARTICLE INFO

Edited by Jing M. Chen

*Keywords:*
Sentinel-1
P-SBAS
Landslide
Fragility curves
Vulnerability curve
Risk

ABSTRACT

The occurrence of landslides can potentially cause considerable economic impact on a global scale, resulting in damage to exposed structures and infrastructures, including buildings. In order to determine the most efficacious risk mitigation strategies, the scientific community is engaged in the analyses aimed at assessing the expected consequences of landslide activation/reactivation. This approach involves the implementation of quantitative risk assessment procedures, based on the definition of the landslide susceptibility and intensity, the identification of exposed elements, and the vulnerability assessment, which represents the most challenging parameter. The present work proposes an approach to the quantitative vulnerability assessment for buildings exposed to slow-kinematic landslides via empirical fragility and vulnerability curves, which express the probabilistic relationship between the damage severity to exposed buildings and the intensity of the landslide. A comprehensive database was compiled, collating information on landslide-induced damage to over four thousand buildings in the Northern Apennines of Central Italy. The landslide intensity is evaluated by exploiting the worldwide freely accessible Sentinel-1 SAR images, which have been processed by using the Parallel-Small BAseline (P-SBAS) – Differential SAR Interferometry (DInSAR) processing chain. The Institute for Electromagnetic Sensing of the Environment (IREA) of the National Research Council (CNR) of Italy is responsible for the processing of the Sentinel-1 SAR images, within the framework of an agreement with the Italian Ministry of Environment and Energy Security (MASE) for the detection and analysis of ground displacement over the entire Italian territory. The ultimate objective of the present study is the exploitation of the derived vulnerability curve into the quantitative risk assessment procedure for a comprehensive evaluation of buildings in the Northern Apennines.

## 1. Introduction

The occurrence of landslides can potentially cause significant damage to exposed structures and infrastructures, including buildings and roads (Castelli et al., 2003). These effects may have both economic and social implication. From an economic standpoint, periodic renovation work may be required, demanding significant costs. From a social perspective, in the most severe cases, the buildings may be deemed inaccessible by the authorities, due to the possible significant negative impact on the lives of the owners. The scientific community is engaged in analyses aimed at estimating the expected consequences resulting from the activation/reactivation of landslides, in order to identify the most suitable risk mitigation strategies, both structural and non-structural (Peduto et al., 2017a). While there has been extensive research on the quantification of landslide hazard, studies on consequence analysis and vulnerability assessment have been relatively limited (Corominas et al., 2013). The evaluation of vulnerability is typically conducted in terms of two different analytical perspectives: the social sciences and the natural sciences (Luo et al., 2023). Social scientists characteristically interpret vulnerability as a series of

☆ This article is part of a Special issue entitled: 'Ten years of Sentinel-1 in space (Invitation Only)' published in Remote Sensing of Environment.

* Corresponding author at: Earth Sciences Department, University of Florence, Via La Pira 4, Firenze, Italy.
*E-mail addresses:* francesco.poggi1@unifi.it, poggi.f@irea.cnr.it (F. Poggi), francesco.caleca@unifi.it (F. Caleca), olga.nardini@unifi.it (O. Nardini), francesco.barbadori@unifi.it (F. Barbadori), matteo.delsoldato@unifi.it (M. Del Soldato), deluca.c@irea.cnr.it (C. De Luca), casu.f@irea.cnr.it (F. Casu), bonano.m@irea.cnr.it (M. Bonano), lanari.r@irea.cnr.it (R. Lanari), veronica.tofani@unifi.it (V. Tofani), federico.raspini@unifi.it (F. Raspini).

https://doi.org/10.1016/j.rse.2025.115199
Received 18 April 2025; Received in revised form 14 August 2025; Accepted 11 December 2025
Available online 18 December 2025

socioeconomic factors that delineate the capacity of individuals or communities to withstand stress and adapt to change (Birkmann, 2013; Blaikie et al., 2014; Fuchs et al., 2012). Conversely, from the standpoint of natural science, the concept of vulnerability is centred on the consequences for the constructed environment, with damage to structures invariably being a key component. In the context of landslide analysis, the term "vulnerability" is used to describe the potential loss of a specific element (or group of elements) exposed to the occurrence of an event of a given magnitude or intensity (Caleca et al., 2022b). It represents the most challenging parameter to be determined within the risk definition (Luo et al., 2023). In recent years, different studies have been conducted with the aim of assessing vulnerability. The majority of the approaches refer to site-specific and local scale analyses, due to the necessity of in-depth knowledge of the characteristics of both landslide (e.g., volume of the displacing mass, kinematics) and exposed facilities (stiffness/strength of constituting materials, state of maintenance, type of foundation, value) (Corominas et al., 2013; Peng et al., 2015). The collection of this relevant information is not a straightforward process subjected to a number of sources of uncertainty (Glade, 2003). The following factors must be considered when investigating landslide vulnerability: the spatial distribution of the intensity parameter and its temporal variability; the resistance of exposed element, which can vary significantly; and the lack of comprehensive databases of damage to facilities and their updating over time. (Peduto et al., 2017a). At wide scale, to face the lack of specific information concerning buildings and landslides, alternative approaches have been developed using the aggregated information available, such as the number of buildings, the percentage of area associated with landslide (Caleca et al., 2022b). Alternatively, in light of the difficulties and uncertainties associated with vulnerability assessment, precautionary approaches adopted its value equal to 1 (Uzielli et al., 2008).

As for other natural hazards, landslide intensity is a pivotal parameter in quantitative risk analysis for the evaluation of vulnerability. Although the definition provided by Hungr et al. (1997) of the landslide intensity as "*a set of spatially distributed parameters determining the destructiveness of a landslide*" is widely accepted (Peng et al., 2015), no unique or standardised methodology exists for quantitatively measuring landslide intensity (Uzielli et al., 2008). Other intensity parameters include total displacement, differential displacement and depth of the sliding surface (Fell et al., 2008). Despite the numerous proposed methodologies, the practical assessment of intensity remains a challenging task due to its site-specific nature (Corominas et al., 2013) and the necessity to consider a multitude of parameters, including geometric and kinematic factors, depending on the landslide type and propagation mechanism. In the case of slow-moving landslides (including large slides, rockslides and earthflows), the intensity is typically expressed in terms of total displacement (Saygili and Rathje, 2009), differential ground deformation (Negulescu and Foerster, 2010) and displacement rate (Frattini et al., 2013; Mansour et al., 2011). These parameters are closely related to the expected degree of damage to urban settlements and general infrastructure. Solari et al. (2018) propose the use of satellite interferometric data for the evaluation of landslide intensity. In recent decades, spaceborne Synthetic Aperture Radar (SAR) has been widely acknowledged as an active remote sensing tool enabling the accurate radar detection of the Earth's surface in all weather conditions, day or night (Bamler and Hartl, 1998). In this regard, monitoring techniques utilising spaceborne Advanced Differential SAR Interferometry (A-DInSAR), also referred to as Multi Temporal Differential SAR Interferometry (MT-DInSAR), may provide valuable insights into displacement patterns experienced by a specific facility or set of facilities situated in (or close to) areas affected by slow-kinematic landslide (Cascini et al., 2013; Ferlisi et al., 2015; Peduto et al., 2017a). The A-DInSAR is a powerful geodetic technique that allows for the accurate measurement of ground displacements from multiple pairs of SAR images acquired over the same area in different times, respectively (Crosetto et al., 2016; Massonnet and Feigl, 1998). In recent years, a considerable number of A-DInSAR techniques have been developed by the scientific community and private companies for the processing of satellite radar acquisitions. A large family of algorithms is currently available for the analysis of extensive sequences of SAR imagery, with the ultimate objective of retrieving Line of Sight (LoS) time series of displacements. Starting from the pioneering Permanent Scatterer Interferometry (PSI) (Ferretti et al., 2001) and the revolutionary Small BAseline Subset (SBAS) (Berardino et al., 2002) algorithms, dozens of different techniques flourished and are currently available, among which the Cross-Track-InSAR (CT-InSAR) (Mora et al., 2003), Stanford Method for Persistent Scatterers (StamPS) (Hooper et al., 2004), SqueeSAR (Ferretti et al., 2011) and Parallel-Small BAseline Subset (P-SBAS) (Casu et al., 2014; Manunta et al., 2019). Due to the high spatial resolution and high accuracy of the measurements, A-DInSAR techniques have been widely employed to map and monitor the surface displacements resulting from geological hazardous events such as landslides (Antonielli et al., 2019; Novellino et al., 2021; Rosi et al., 2018) and land subsidence (Osmanoğlu et al., 2011; Solari et al., 2018). In this framework, a key role is played by the Sentinel-1 mission of the European Copernicus programme that, starting from 2014, provides the systematic acquisition of C-band radar data (wavelength 5.5 cm and incidence angle ranging from 33° to 43°) with a short revisit time (12 or 6 days in the case of one or two operating satellites, respectively), and with free and open access data policy and a small orbital "baseline tube" (with a 200 m nominal diameter) that ensures the reliability and soundness of DInSAR applications (Torres et al., 2012).

In this work we extensively exploit Sentinel-1 A-DInSAR products to provide a quantitative assessment of landslide vulnerability based on empirical fragility and vulnerability curves. The aforementioned curves are indicative of the probabilistic relationship between the severity of the damage and the intensity of the landslide, focusing on structural elements exposed to slow-kinematic landslides. More in detail, the fragility curves indicate the probability of exceeding a given level of damage for a range of landslide intensity values (Mavrouli et al., 2014). From those ones, the vulnerability curve is derived, which provides the relationship between the mean level of damage severity to a given building or aggregate of buildings and the landslide intensity value (Peduto et al., 2017a), expressing the vulnerability of buildings in probabilistic terms, incorporating uncertainties (Mavrouli et al., 2014). The outcome provides a quantitative assessment of building vulnerability, utilising a numerical index that ranges from 0 (no degree of loss) to 1 (total degree of loss).

### *1.1. Fragility curve: State of art*

A review of the existing scientific literature on approaches for the generation of fragility curve for landslide analysis was performed using the freely accessible "Web of Science" (WoS) (Clarivate, 2019). The WoS database for natural sciences and engineering is comparable to the Scopus search engine, both of which offer comprehensive coverage of journals, articles, and cited reference levels (Norris and Oppenheim, 2007). The WoS has previously been employed with considerable success in the context of both landslide (Mondini et al., 2021) and subsidence (Raspini et al., 2022) research.

The WoS website offers an advanced search functionality, which allows users to set specific parameters to conduct more precise research. The specific criteria for data collection are outlined in the following section. The Topic (TS) command allows enables the extraction of target contributions, whereby words included in the title of the paper, abstract, or list of author keywords are identified. In this field, the following terms were employed: "*Fragility curve*" and "*Landslide*" related by the Boolean operators, i.e. "*AND*", to combine the various terms into a single condition. The conditions adopted for the present work are as follows:

$$\left(TS = \text{"}Fragility\ curve\text{"}\right)\ AND\ \left(TS = \text{"}Landslide\text{"}\right)$$

The data collection was conducted in October 2024 and results into a preliminary list of 75 contributions. Of the aforementioned contributions, 6 do not address the direct generation of fragility curves, 11 pertain to congresses, conferences, or symposia (and then they are non-accessible), and one refers to a review of the building vulnerability to landslides (Luo et al., 2023). The remaining 57 papers, whose topic focus includes both fragility curves and landslide can be grouped in two different main approaches. The first approach, recognizable in 46 papers, addresses the modelling of landslide fragility curve according to two main categories of geohazard: *i)* the first category comprises 24 papers that employ modelling to investigate landslides triggered by earthquakes (Fotopoulou and Pitilakis, 2013); *ii)* the second category includes 22 papers that utilise numerical modelling to examine rainfall-induced landslides (Parisi and Sabella, 2017). The second approach, considering the empirical interaction between structures or infrastructures and landslides to the generation of fragility curves, is explained in 11 papers. This paper adopts a methodology similar to that described in the latter group of papers. The most pertinent literature included in this group is listed in Table 1 for reference. The analysis of the state-of-art indicates that local-scale analyses are the preferred method for vulnerability assessment when detailed, high-precision information is available.

This review highlights that vulnerability is still the most critical parameter to be determined within the chain of the landslide quantitative risk assessment and the absence of a standardised methodology. In this paper, the efforts of the authors have been focused on the development of an innovative, scalable and transferable procedure, exploiting the large availability of A-DInSAR datasets, to determine building vulnerability to slow-moving landslide at wide scale.

## 2. Proposed procedure

The present paper proposes a procedure for the quantitative assessment of the vulnerability in buildings affected by slow-kinematic landslides, employing the construction of fragility and vulnerability curves. The purpose is the introduction of a quantitative vulnerability values into the quantitative risk assessment (QRA) procedure for each building, defined through the risk equation:

$$R = H^{*}V^{*}E \tag{1}$$

where $R$ is the landslide risk, expressed as the expected monetary loss to exposed elements; $H$ is the hazard, indicating the spatial and temporal probability of landslide occurrence; $V$ is the vulnerability, describing the expected degree of loss of exposed elements and $E$ is exposure, representing the economic value of exposed elements. As delineated in the flowchart in Fig. 1, the proposed QRA procedure comprises a three-phase vulnerability assessment.

The initial step, *Phase I*, is the collection of data entailing the identification of target areas for subsequent field activities and damage surveys. Vulnerable areas are identified by utilising on the Italian landslide inventory map (IFFI, "*Inventario dei Fenomeni Franosi in Italia*") and the Sentinel-1 A-DInSAR datasets, both of which are available at a national scale and exhibit homogeneous characteristics. The IFFI was developed by the Italian Environmental Protection and Research Institute (ISPRA, "Istituto Superiore per la Protezione e la Ricerca Ambientale") in collaboration with regional authorities and provinces (Trigila et al., 2010). It provides a comprehensive overview of landslide distribution across the whole Italian territory, accompanied by a database of polygons delineating the typology and extent of landslide-affected areas (Iadanza et al., 2021). The ground deformation dataset comprises a national coverage of measurement points (MPs) acquired in both ascending and descending orbits through the analysis of Sentinel-1 data processed via the P-SBAS processing chain. The data pairs employed in the generation of the interferograms are distinguished by a minimal spatial separation between the orbits (baseline), with the objective of limiting the effects of spatial decorrelation (Lanari et al., 2004). The A-DInSAR technique represents the most advanced tool for wide-area deformation measurement to date, being particularly suitable for application in urbanised areas, which are the target of the analysis. The urban fabric of small Italian hamlets situated in the Northern Apennines is characterised by a sparse and discontinuous arrangement of buildings, with expansive forest areas situated between them. The hamlets are constituted by adjoining or terraced buildings, the majority of which were constructed during the nineteenth and early twentieth centuries.

The activities conducted during *Phase II* are twofold: firstly, to carry out field surveys in vulnerable areas for the purpose of damage severity classification; secondly, to post-process the A-DInSAR datasets for the definition of a robust intensity parameter, based on deformation data. The approach proposed by Del Soldato et al., 2017 was employed for the classification of landslide-induced damage. A notable advantage of this approach is that it does not require the visualization of foundations or the internal spaces of structures. The damage assessment is subdivided into two phases. The first phase is the classification of landslide-induced damage that can be observed on structures and infrastructure. The second phase involves a categorisation of the overall structure depending on the severity and extension of damage that was previously identified.

As delineated by Del Soldato et al. (2019), the cracks and fractures observed in structures and infrastructures can be classified into six distinct categories based on their characteristics: *i*) *No damage*, undamaged building; *ii*) *Negligible*, thin and isolated cracks with a width of less than 1 mm; *iii*) *Weak*, distortion and tilting of the structure, which does not impact its stability, and cracks with a width lower than 5 mm; *iv*) *Moderate*, the presence of cracks with width lower than 15 mm, which begin to influence the strength of the structure; *v*) *Severe*, the presence of spread cracks and fractures, with widths lower than 25 mm, that conditioning the resistance of the structure; and *vi*) *Very severe*, the partial collapse of floors, with width of cracks greater than 25 mm. In addition to the severity of the damage, the number of cracks is taken into consideration. The information on the severity and extent of damage can be combined using a matrix for the classification of the structure in eight classes, in order to be comparable with other existing approaches: *i) No damage, ii) Negligible, iii) Weak, iv) Moderate, v) Serious, vi) Very serious, vii) Potential collapse, and viii) Unusable*. Subsequently, these categories were regrouped into three categories to facilitate the construction of fragility curves: *i)* D1 represents *No damage*, *Negligible* and *Weak*; *ii)* D2, *Moderate* and *Serious*; and *iii)* D3, *Very serious*, *Potential collapse* and *Unusable*.

The A-DInSAR datasets available at the national scale encompass both the horizontal (East-West) and vertical (up-down) components. Thus, the data are employed to establish a reliable deformation intensity parameter through the definition of the modulus of the deformation (eq. 2), which overcomes the issue of the direction of deformation:

**Table 1**
List of papers deal with empirical modelling of damage to structures of infrastructures caused by slope instability.

| Papers | Exposed elements | Location | Extension |
|---|---|---|---|
| Del Soldato et al., 2019 | *Buildings* | *Patigno and Coloretta hamlets (Zeri, Italy)* | *Site-specific* |
| Ferlisi et al., 2018 | *Buildings* | *Lungro and Verbicaro (Cosenza, Italy)* | *Site-specific* |
| Ferlisi et al., 2019 | *Buildings* | *Lungro and Verbicaro (Cosenza, Italy)* | *Site-specific* |
| Ferlisi et al., 2021 | *Road networks* | *Cilento (Italy)* | *Extended* |
| Nicodemo et al., 2016 | *Buildings* | *Lungro and Verbicaro (Cosenza, Italy)* | *Site-specific* |
| Peduto et al., 2017a | *Buildings* | *Lungro and Verbicaro (Cosenza, Italy)* | *Site-specific* |
| Peduto et al., 2017b | *Bridges* | *Netherlands* | *Extended* |

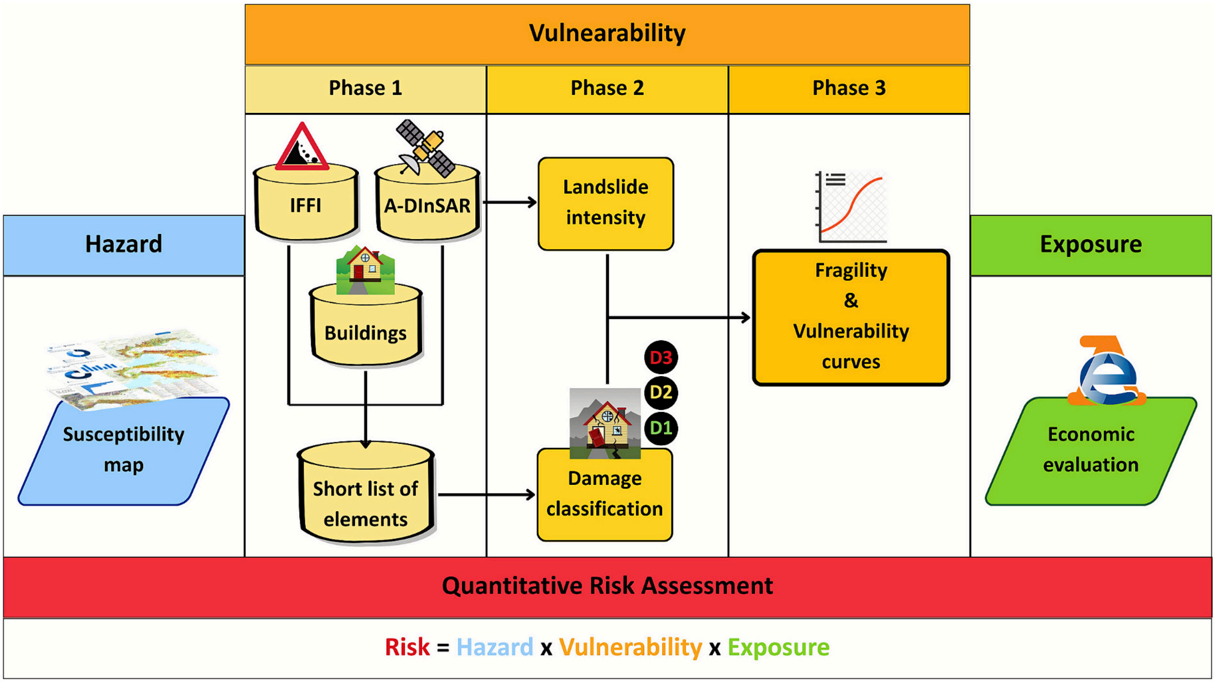


**Fig. 1.** – Flowchart of the proposed procedure for the quantitative vulnerability assessment of buildings detailing each step involved in the identification of exposed elements (phase 1), evaluation of damages and landslide intensity (phase 2), and construction of the fragility and vulnerability curves (phase 3). The outcome fits within the QRA procedure.

$$V_{modulus} = \sqrt{V^2_{horizontal} + V^2_{vertical}} \tag{2}$$

In *Phase III*, the damage severity data collected for each building inspected during the surveys are merged with the intensity values derived from the A-DInSAR dataset. One of the principal constraints associated with A-DInSAR measurements is the discontinuous coverage of the information. Consequently, only those buildings with a measurement point situated within a radius of 50 m are assigned an intensity value. The newly generated dataset is then employed for the construction of fragility and vulnerability curves, in accordance with the procedures proposed by Fotopoulou and Pitilakis (2013) and Mavrouli et al. (2014). The concept of fragility curves is well established in the context of earthquake-threatened buildings, with a number of mathematical procedures for their development proposed in the scientific literature. The fragility curves for landslides express the probability of exceeding a given damage level, for a range of values of landslide intensity parameters, in a single diagram (Mavrouli et al., 2014), calculated as follows:

$$P(Damage \geq D_i|\Delta) = \phi\left[\frac{1}{\beta}\ln\left(\frac{\Delta}{\overline{\Delta_i}}\right)\right] \; (i = 1, 2, 3) \tag{3}$$

in this context $\phi[.]$ represents the standard normal cumulative distribution function, $\Delta$ is used to indicate the intensity parameter, while $\overline{\Delta_i}$ denotes the median value of the intensity parameter at which the building reaches the damage ($i$) severity level. Additionally, β is the standard deviation of the natural logarithm of the intensity parameter.

For each of the $\Delta$ values obtained from the analysis of A-DInSAR data pertaining to the sample of vulnerable areas, the corresponding fragility curves were used to compute $\mu_D(\Delta)$ according to the formula adapted from (Fotopoulou and Pitilakis, 2017):

$$\mu_D(\Delta) = \sum_{i=1}^{3} P_i{}^*d_i \tag{4}$$

where, $P_i$ is the discrete probability associated to the damage severity level ($D_i$) whose numerical index equals $d_i$ (taken for this application as 1, 2 and 3 for $D_1$, $D_2$, and $D_3$, respectively).

The vulnerability curve for the study area is recovered according to the procedure described by Giovinazzi and Lagomarsino (2004) and Peduto et al. (2017a), whereby the fragility curves $(\mu_D(\Delta), \Delta)$ are fitted with the equation:

$$\mu_D = a^*[b^*\tanh(c^*\Delta + d)] \tag{5}$$

where, $\mu_D$ the weighted average of the damage severity levels for a given value of the intensity parameter ($\Delta$), whereas the four coefficients, $a$, $b$, $c$, and $d$, must be determined by a curve fitting. A unique equation of vulnerability curve has been derived which correlates the intensity with vulnerability values.

This result is incorporated into the QRA procedure for risk assessment (Eq. 1). The hazard ($H$) represents the spatial and temporal probability of landslide occurrence. The retrieval of suitable data for evaluating temporal probability of occurrence, usually quantified as frequency, return period or exceedance probability, is challenging, especially when dealing with analysis at wide scale. Therefore, the spatial probability of occurrence, expressed as susceptibility, was adopted to quantify this parameter. (Caleca et al., 2022b). The decision serves to reduce the complexity of the problem. Nevertheless, as asserted by Corominas et al. (2013), the assessment of landslide susceptibility can be regarded as an end product in itself, which can be applied in land-use planning and environmental impact assessment. This is particularly pertinent where insufficient data is available to assess the spatial and temporal probabilities of events, as highlighted by Caleca et al. (2022b). Accordingly, the hazard is approximated with an index derived from previous landslide susceptibility studies, in particular, by exploiting the product provided by Trigila et al. (2013). The susceptibility probabilities are modelled by using the Random Forest algorithm (Breiman, 2001), which have been trained on data from the IFFI inventory and several environmental parameters (e.g. slope, curvatures, aspect, rainfall data, lithological data). This approach attempts to predict continuous values on a scale of 0 to 1, expressing the percentage of area affected by landslides. The vulnerability ($V$) is derived directly from the equation of the vulnerability curve for those buildings in the proximity of which an A-DInSAR measuring point is situated. Finally, the exposure ($E$) has been evaluated using the *Osservatorio Mercato Immobliare* (OMI) database, which is maintained and reviewed by the National Revenue Agency. The database encompasses the trade prices (in euros per square metre) for buildings, which have been aggregated at the municipal level. Subsequent to the implementation of the QRA procedure, a quantitative value is assigned to each building within the designated area of study in terms of its hazard, its vulnerability and its exposure, as previously explained. The multiplication of these values allows for the quantitative assessment of landslide risk, in economic terms, associated with each building.

## 3. Study area and available datasets

The Northern Apennines, Central Italy, covers an area of over 41,000 km$^2$, and was selected for the implementation of the methodology due to the prevalence of slow-moving landslides within this region, depending on the bedrock lithology and landscape morphology (Segoni et al., 2014), which have pervasively shaped the landscape. Fig. 2 illustrates the IFFI landslide inventory, which is the most comprehensive and accurate landslide database currently available in Italy.

Within the IFFI inventory, landslides are represented at different levels of detail, categorised as follow: *i) punctual* (PIFF) is the landslide identification points; *ii) linear*, which contains those phenomena whose length greatly exceeds their width and which are so small that they cannot be mapped at a scale of 1:25,000; and *iii) areal*, landslides mapped by a polygon. In this study, the focus is on the landslides represented by a polygon, which encompass more than 620,000 landslides at national scale over an area of approximately 24,000 km$^2$, representing 7.9 % of the Italian territory. With more than 200,000 mapped landslides, covering an area of 5649 km$^2$, the Northern Apennines represent one of the most prone to slope instability regions in Italy. In order to enhance the visual representation, the landslides are classified according to the type of movement observed and grouped into three principal categories based on the predominant kinematics. The slow movement category comprises: *i) rotational/translational slide*, *ii) lateral spread*, *iii) slow earth flow*, *iv) complex*, *v) DSGSD* (Deep-Seated Gravitational Slope Deformation), and *vi) n.d.* (not defined) movement. The rapid movement category encompasses: *i) rapid debris flow,* and *ii) area affected by numerous shallow landslides*. The fall movement category comprises: i) *rockfall/topple,* and *ii) area affected by numerous rockfalls/topples*.

In this scenario, the adoption of satellite interferometric techniques to map ground deformation represents the most suitable solution. The A-

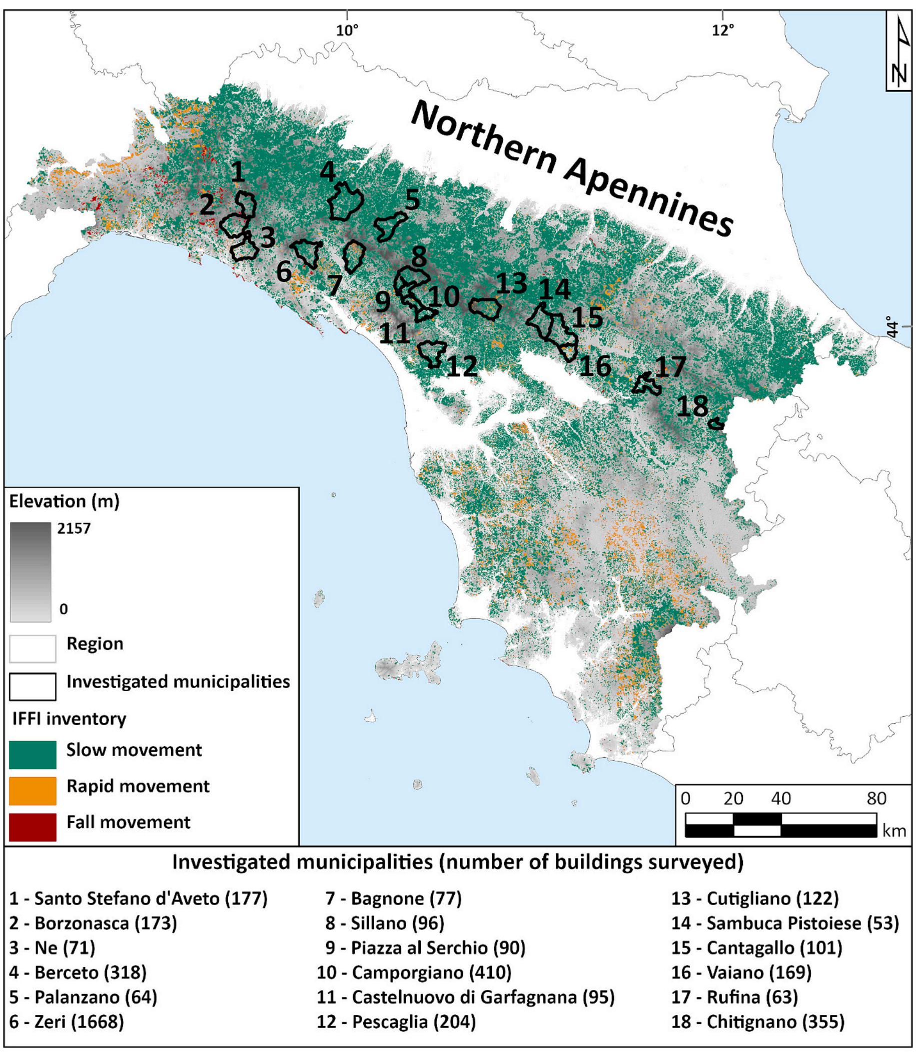


**Fig. 2.** – The area of interest in the Northern Apennines, where the slope exceeds 5°, is delineated by the digital elevation model (TINITALY DEM) with tones from bright brown to darken brown. The landslides in the IFFI inventory are grouped according to their predominant kinematic movement: in green tone the slow-moving landslide; in orange tone the rapid movement; and in red tone the rockfall. The black polygons delineate the municipality boundaries that were investigated in the area of interest. For each municipality is reported also the number of buildings investigated, further information is available in the Appendix. (For interpretation of the references to colour in this figure legend, the reader is referred to the web version of this article.)

DInSAR dataset was produced by the Institute for Electromagnetic Sensing of the Environment (IREA) of the National Research Council (CNR) of Italy within the agreement with the Italian Ministry of Environment and Energy Security (MASE) for the detection and analysis of ground displacements and the corresponding mean velocity maps over the entire Italian territory. This operational service, based on the P-SBAS algorithm (Manunta et al., 2019), is fully automatic and unsupervised, and it supports the Italian public institutions with large-scale surface deformation monitoring at national scale. As illustrated in Fig. 3, the implemented P-SBAS processing chain exploits Sentinel-1 SAR data acquired from both ascending and descending orbits, thereby permitting the retrieval of the vertical and horizontal (East-West) components of the surface displacements. In order to ensure the reliability of the displacement measurements, only pixels exhibiting temporal coherence (Pepe and Lanari, 2006; Onorato et al., 2025) with a value exceeding 0.9 (Manunta et al., 2019) were retained for the purposes of the monitoring service. To achieve these results, the entire SAR dataset relevant to the Italian territory is partitioned, starting from June 2016, into stacks of data subsets that can be independently processed to first retrieve the LOS measurements and then, the vertical and horizontal displacement components. Specifically, for both the ascending and descending orbits, 19 and 17 stacks, respectively, are generated (see Fig. 3). The processing information pertaining to Sentinel-1 P-SBAS is listed in Table 2 and further elaborated in Manunta et al. (2019). It is noteworthy that, following the independent processing of P-SBAS for each of the 36 datasets, the retrieved LOS displacement time series and the corresponding mean deformation velocity maps are relative to distinct reference points. This represents a significant constraint for the phase unwrapping procedure, as outlined in Pepe and Lanari (2006). Starting from the LOS displacements retrieved over ascending and descending orbits, the vertical and horizontal components are achieved by applying the algorithm detailed in (De Luca et al., 2017). This algorithm describes a suitable procedure for estimating large-scale displacement components solving the issue relevant to the different LOS reference points.

**Table 2**
– Summary table of the parameter employed in the P-SBAS processing chain of the Sentinel-1 imagery.

| | P-SBAS processing chain | |
|---|---|---|
| *SAR imagery* | Sentinel-1 A / Sentinel-1B | |
| *Band* | C | |
| *Sensor mode* | IW | |
| *Acquisition geometries* | Ascending | Descending |
| *Time range in analysis* | 06/2016–11/2023 | |
| *DEM used* | SRTM-1 arcsec | |
| *LOS pixel spacing* | ≈ 70 m | |
| *Component pixel spacing* | ≈ 30 m | |
| *Spatial and temporal baseline for P-SBAS analysis* | 300 days | 200 m |
| *Temporal coherence threshold* | 0.9 | |

The mean deformation velocity maps for the vertical and horizontal components of the entire Italian territory have been obtained, and these comprise over 64 million MPs. Of these, 15 million MPs are located within the area of the Northern Apennines. As illustrated in Fig. 4, insights into the displacement components within the Northern Apennines area (see Fig. 2) are presented, encompassing both the horizontal (A) and vertical (B) components. It is important to highlight that to allow a combination of the LOS analysis, the P-SBAS results are geocoded onto a common geographic grid, in this case the SRTM-1 arcsec is used as reference, thus obtaining a pixel spacing of the vertical and horizontal displacement components of about 30 m.

As previously stated, the implementation of the QRA procedure across the Northern Apennines region is contingent upon the availability of information regarding landslide susceptibility, which is necessary for the delineation of landslide hazard. Fig. 5A presents the landslide susceptibility map of the Northern Apennines, which utilises the product provided by Trigila et al. (2013). The susceptibility is defined as a probability model, which is dependent on several environmental parameters (e.g. IFFI inventory, slope, curvatures, aspect, rainfall data,

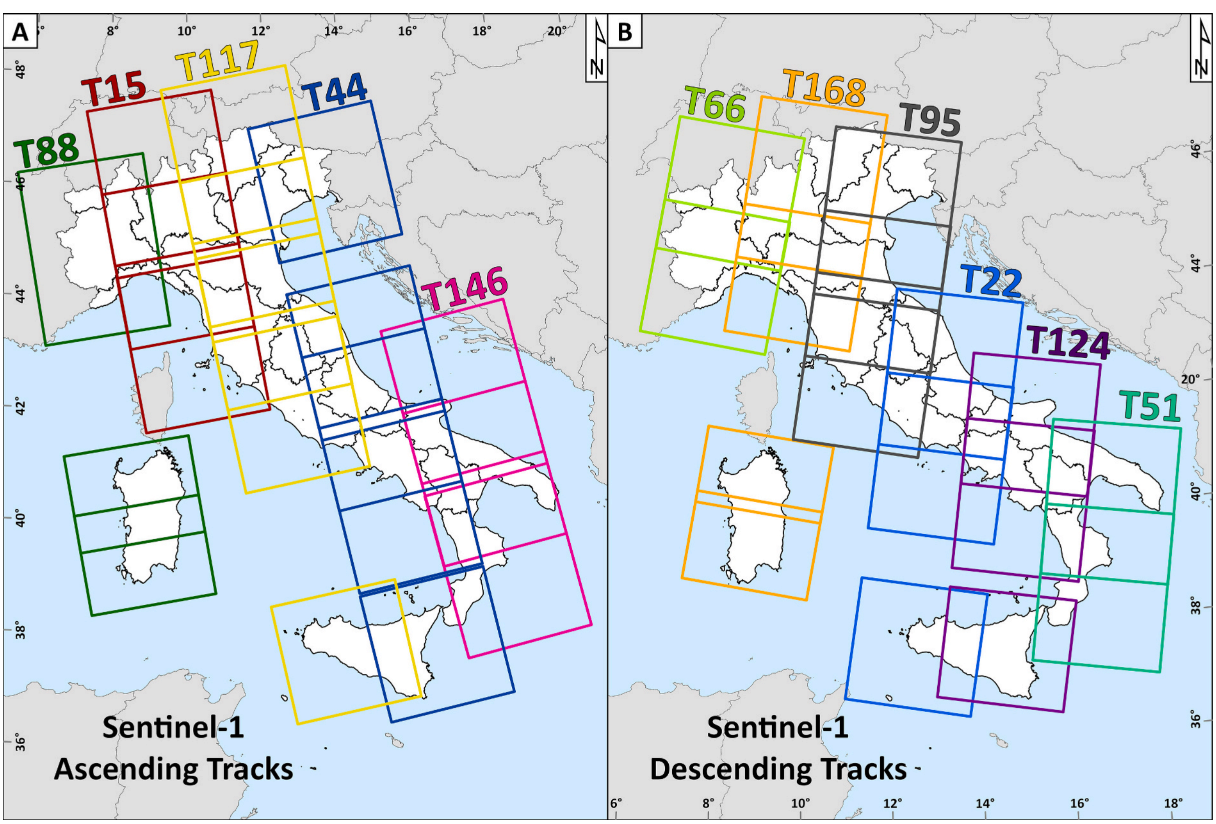


**Fig. 3.** – The Sentinel-1 footprint tracks in ascending (A) and descending (B) geometries over the Italian territory.

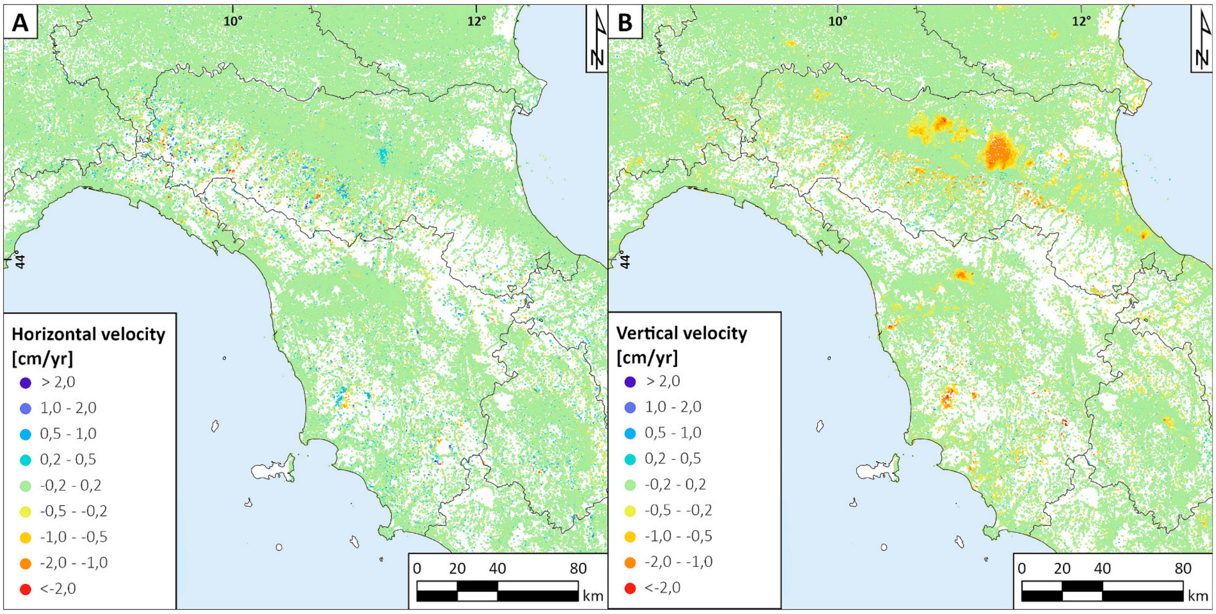


**Fig. 4.** – The A-DInSAR datasets at the national scale processed via the P-SBAS algorithm, exploiting the Sentinel-1 SAR images in both A) horizontal, and B) vertical components. The black lines delineate the regional boundaries within the Italian territory.

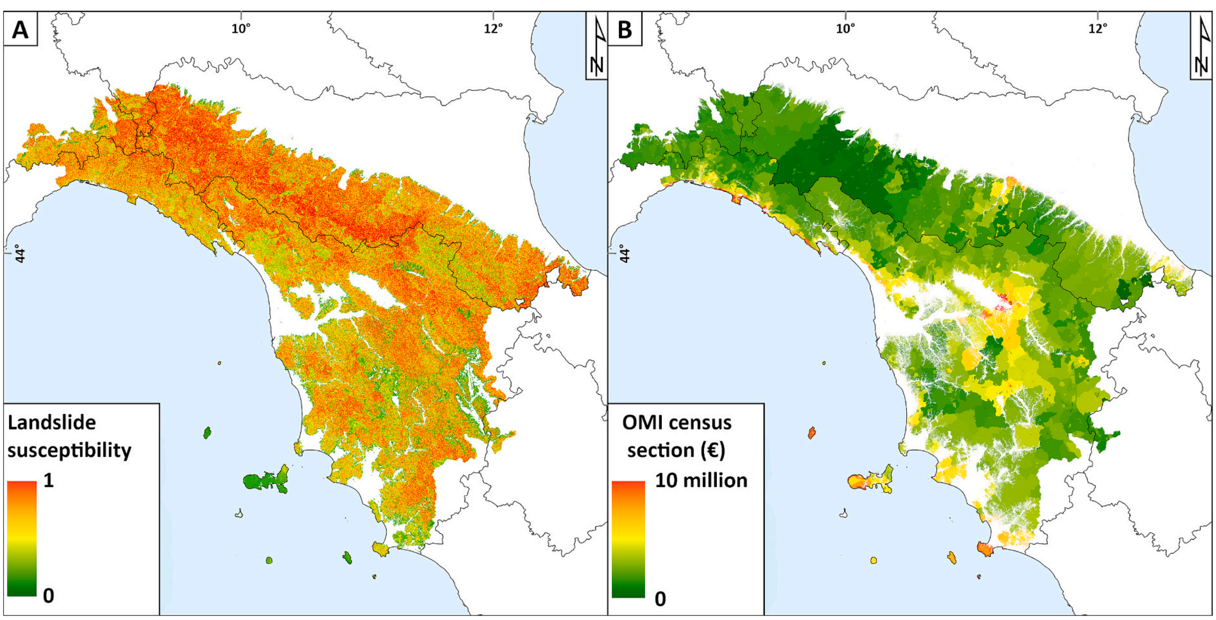


**Fig. 5.** - For the area of interest in the Northern Apennines: A) Landslide susceptibility map, and B) OMI census section, in which each census expresses the economic valuation in Euro per square meter of buildings in the municipality. The black lines delineate the regional boundaries within the Italian territory.

lithological data). As Fig. 5A illustrates, the areas in which surveys are conducted to catalogue landslide-induced damage to buildings are characterised by a high susceptibility, represented by tones of orange to red. Additionally, data from the OMI database, which is characterised by the economic valuation per square metre, is necessary for the delineation of the exposure of buildings. In Fig. 5B illustrates the census section of the Northern Apennines. It is evident that the highest value corresponds to the location of the largest urban centre (Florence, Genoa, etc.), while values in mountainous areas are comparatively low. In addition, it is important to note the exclusion of areas exhibiting an absence of landslides as a geomorphological phenomenon (i.e., alluvial plains and flat areas) from the computational framework.

## 4. Generation of fragility and vulnerability curves

A comparative analysis of the A-DInSAR datasets with the IFFI inventory and build-up areas has enabled the selection of 18 municipalities in the Northern Apennines for field surveys aimed at quantifying the damage caused by landslides to buildings. The selected municipalities are distributed across three regions (Figure 2Figure 4): *i)* Tuscany, represented by the municipality of Bagnone, Camporgiano, Cantagallo, Castelnuovo di Garfagnana, Chitignano, Cutigliano, Pescaglia, Piazza al Serchio, Sambuca Pistoiese, Sillano, Rufina, Vaiano and Zeri; *ii)* Liguria, including Santo Stefano d'Aveto, Borzonasca, and Ne; and *iii)* Emilia-Romagna, with Berceto and Palanzano.

In the years 2021 and 2022, surveys in areas of study have been conducted, with the objective of cataloguing landslide-induced damages. This objective was achieved by applying the methodology proposed by Del Soldato et al. (2017). A total of 4306 buildings were inspected during the surveys, and their damage information was collected. The damage was classified according to the following categories: *i)* No Damage (226 units), *ii)* Negligible (1294 units), *iii)* Weak (1090 units), *iv)* Moderate (974 units), *v)* Severe (407 units), *vi)* Very Severe (188 units), *vii)* Potential Collapse (78 units), and *viii)* Unusable (49 units). A detailed overview of these categories is provided in Appendix A. The intensity of deformation is defined by calculating the modulus of the A-DInSAR components for the entire Northern Apennines region applying the specified Eq. (2). This is a relatively straightforward task, as for each MPs in the horizontal component, there is a corresponding pair in the vertical component, thus ensuring the number of MPs is preserved. These pairs of data, comprising damage severity and deformation intensity, constitute the fundamental elements for the generation of fragility and vulnerability curves.

In order to provide further insight into the aforementioned datasets, the case of the hamlet of Patigno in the municipality of Zeri (Tuscany) is reported (Fig. 6). This is of particular interest as the entire hamlet is situated on an active landslide, located within the hydrographic basin of the Gordana river (Federici et al., 2001). The Patigno landslide is a large mass movement in the Northern Apennines, extending for a total length of 1.5 km with an average slope of approximately 10°. The landslide has experienced several events of reactivation, which have resulted in the dismantling of the main body into numerous minor landslides. Furthermore, the landslide has been observed to reactivate on numerous times, with the most recent documented events occurring in 1970, 1972, 1975, 1982–1983, and 1993 (Chelli and Stefanini, 1999). The reactivations have resulted in considerable damage to structures and infrastructure. The A-DInSAR analysis provided corroboration of the ongoing activity of the landslide, characterised by a deformation intensity ranging from 1 cm/year in the northern zone (the source area) to over 2 cm/year in the southern portion (the landslide toe). The survey investigation has revealed the occurrence of multiple areas exhibiting severe damage to buildings, particularly in the lowest portion. The church of San Lorenzo, located in the southern portion of Patigno, has experienced structural deterioration, as evidenced by the collapse of the ceiling and the subsequent uninhabitability of the building for approximately three decades (Fig. 6). Additionally, a masonry building in the central area of the hamlet exhibits extensive open fractures across its entire surface.

The damage severity data gathered during the surveys and the deformation intensity derived from the A-DInSAR data were employed to construct the fragility and vulnerability curves in accordance with the methodology outlined by (Peduto et al., 2017a). The damage classes are grouped into the three principal categories: *i)* D1 (2610 units), *ii)* D2 (1381 units) and *iii)* D3 (315 units). The deformation intensity of each building is associated with the nearest measuring point, within a maximum distance of 50 m. This distance was selected in relation to the A-DInSAR spatial resolution, which is approximately 30 m.

The Eq. (4) was applied to define the probability, resulting in fragility curves (Fig. 7A), in green for class damage D1, in yellow for D2 and in red for D3. These curves depict the probability of a given event occurring as a function of the intensity of deformation. For example, an

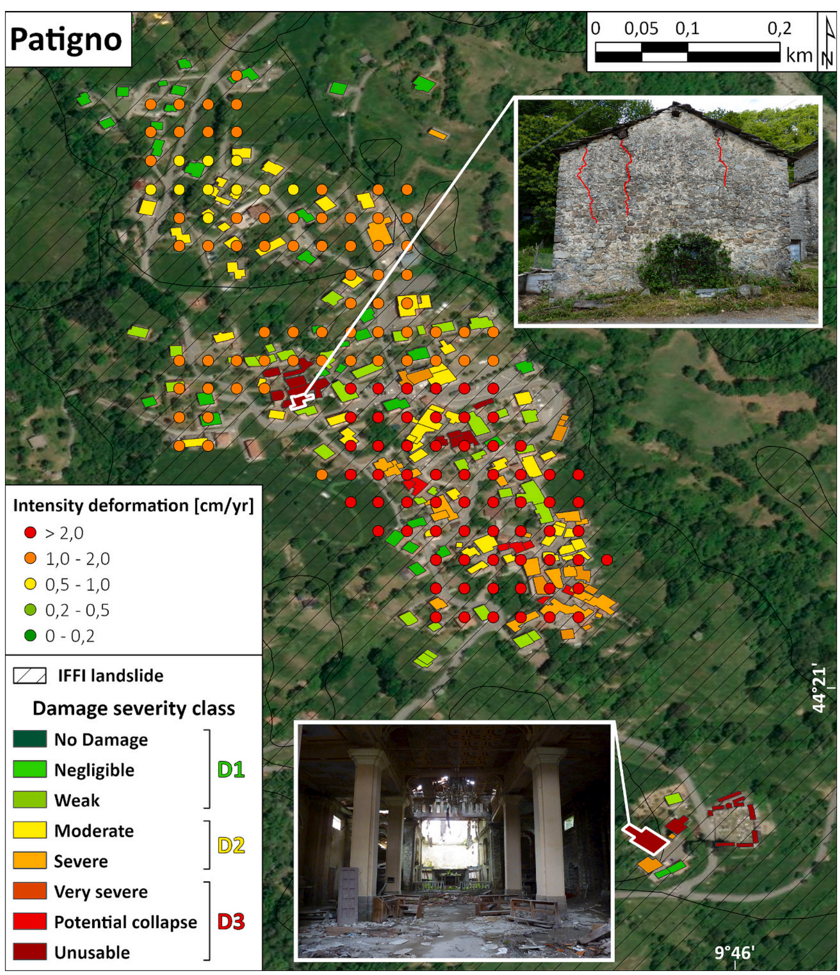


**Fig. 6.** - The severity damage map and the deformation intensity dataset of Patigno hamlet in the municipality of Zeri. The photographs report the damages surveyed during the field investigation in the center of Patigno and in the toe of the landslide, where the collapsed church of San Lorenzo is located.

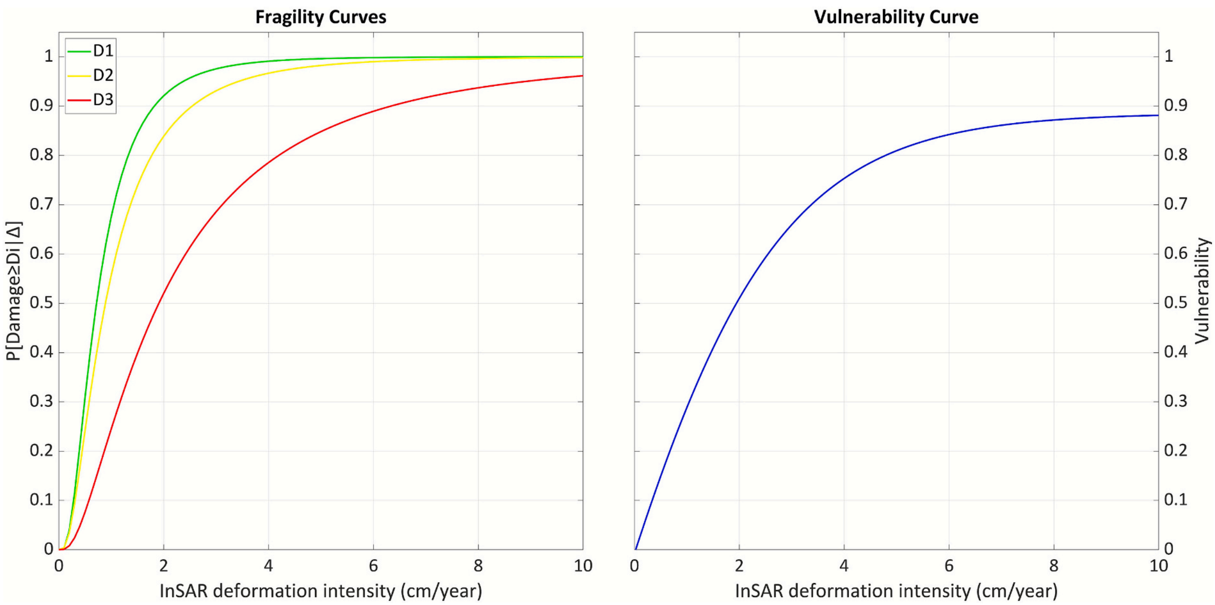


**Fig. 7.** - A) The empirical fragility curves illustrate the damage probability for each velocity interval: D1 (in green); D2 (in yellow); and D3 (in red); B) The empirical vulnerability curve (in blue) for buildings in Northern Apennines. (For interpretation of the references to colour in this figure legend, the reader is referred to the web version of this article.)

examination of a construction in the Northern Apennines with an intensity of 1 cm/yr reveals that the fragility curves permit the a priori prediction of a probability of 0.66 (66 %) for the occurrence of slight damage that does not affect the stability of the building (D1). The probability of encountering moderate or serious damage, which would necessitate repair (D2), is 0.60 (60 %). Ultimately, the probability of encountering very serious damage, which could potentially render the dwelling uninhabitable (D3), is 0.28 (28 %). Subsequently, the Eq. (5) was employed to define the vulnerability, thereby yielding the vulnerability curve illustrated in Fig. 7B. The four coefficients of Eq. (6) are determined by the curve fitting ($a = 0.3666; b = 1.7388; c = 0.0622; d = 0.0213$), and the coefficient of determination ($R^2 = 0.9818$) indicates the accuracy of the regression. The curve depicts the vulnerability of a building to slow-kinematic landslides, delineating the relation between the degree of damage sustained by a given building (or group of buildings) and the corresponding intensity of landslides. A comparable analysis of the aforementioned building reveals a vulnerability value of approximately 0.36 (36 %).

## 5. Application: Quantitative risk assessment in Northern Apennines

The vulnerability curve resulting from this study was subsequently employed in the QRA procedure for the Northern Apennines. In particular, it was assumed that landslide processes generally occurred on slopes exceeding 5° (Tomás et al., 2019). Consequently, only the hilly/mountainous areas were subjected to analysis, utilising the topographical information available through the freely available TINITALY digital elevation model (Tarquini and Nannipieri, 2017). This encompassed a total surface area of 31,000 km$^2$, representing approximately 75 % of the total area of the Northern Apennines (Fig. 2). As a result of this selection process, the majority of the main alluvial plains were excluded from the analysis, as the Florence-Prato-Pistoia plain, which is characterised by a high degree of urbanisation and population density. However, these plains are not susceptible to gravitational phenomena, but rather to processes such as subsidence and uplift (Del Soldato et al., 2018; Festa et al., 2022).

Of the 200,000 mapped landslide in the area of study, 183,000 (91.5 %) are slow-moving landslides that could be effectively monitored and analysed using A-DInSAR techniques (Raspini et al., 2019). This represents a total surface area of 5649 km$^2$, which constitutes 18.2 % of the total area. Furthermore, the freely available online topographic database OpenStreetMap (OSM) (Haklay and Weber, 2008) was utilised to obtain the polygons of more than 1.1 million buildings distributed within the area of analysis. As detailed in the section "Proposed procedure", the QRA procedure is based on the parameters of hazard, exposure, and vulnerability, which are defined for each building. Subsequently, this value was then multiplied by the area of the polygon to obtain the total building exposure. The total estimated exposure for the Northern Apennines is approximately 148 billion euros. It should be noted that the lack of information regarding the number of floors or the height of buildings represents a significant limitation. The vulnerability assessment was conducted directly from the vulnerability curve. The A-DInSAR coverage represents a further limitation to the procedure, in that there are areas not covered, resulting in a reduction of the number of buildings in the analysis to 700,000. Subsequently, for this large subset of buildings, it was enabled to assess the risk through the application of the Eq. (1). The total assessed risk, in terms of economic loss, for the Northern Apennines is approximately 1.8 billion euros.

A comprehensive examination of the outcomes yielded by the QRA methodology is made for the hamlet of Patigno (Fig. 8). For each building, the assessment encompasses the hazard (Fig. 8A), vulnerability (Fig. 8B), exposure (Fig. 8C), and risk (Fig. 8D), respectively. In the case of Patigno, the hazard and vulnerability are high due to the presence of the active landslide that affects the entire hamlet. Conversely, the exposure of the buildings is very low, as would be expected in a remote and mountainous hamlet.

Consequently, the risk assessment is found to be heterogeneous, depending on the corresponding exposure value. Fig. 9 provides a comprehensive overview of the quantitative landslide risk assessment of buildings on the regional scale, aggregated at municipal level. For each municipality in the Northern Apennines, the total risk is defined as the sum of all the risks assessed for the buildings. The average risk for the municipalities is 2.2 million euros, with the highest value of 48 million euros being recorded for the municipality of Genoa, which is the spatially largest city in the area of study and thus represents an outlier compared to the others.

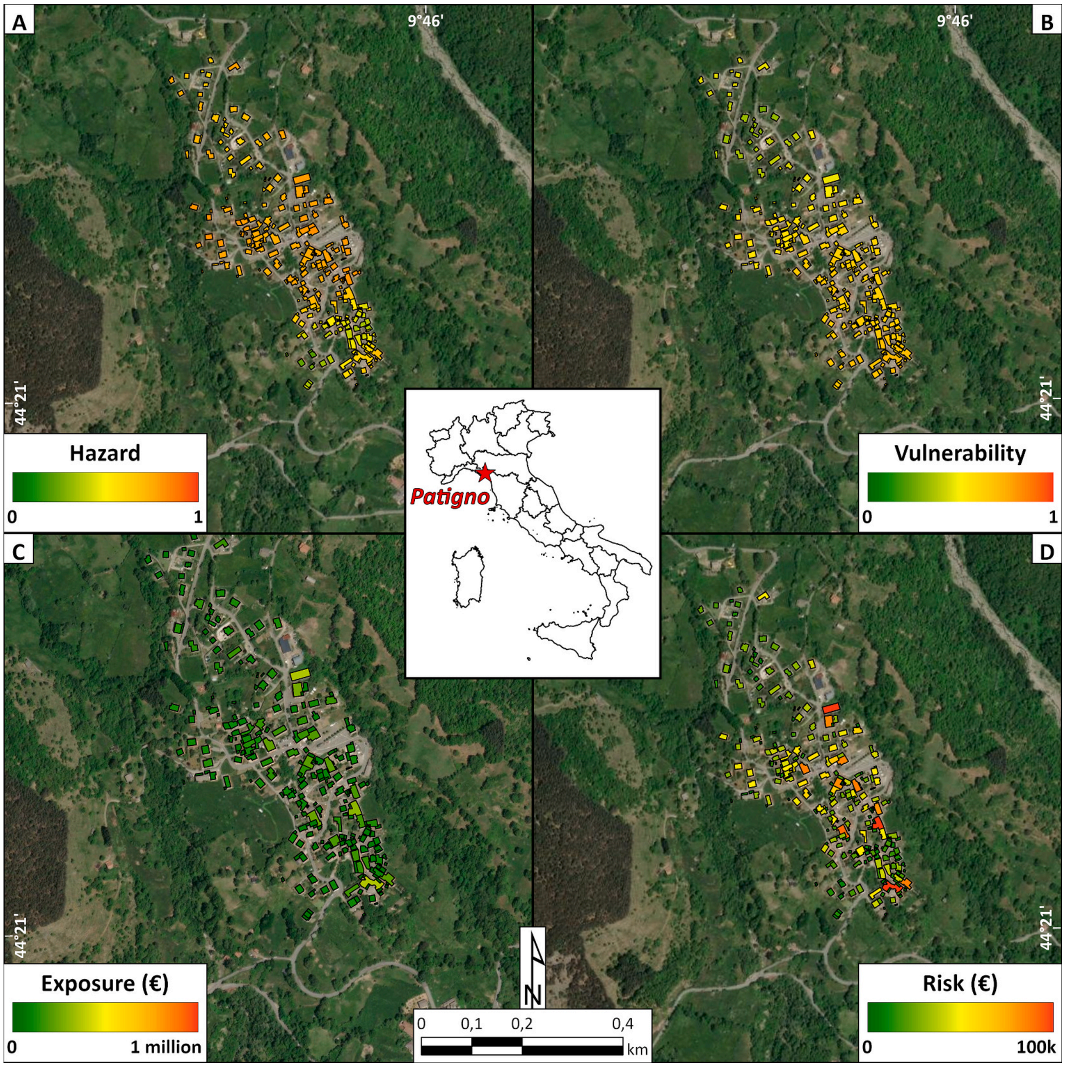


**Fig. 8.** – Visual representation of the resulting parameters in the QRA procedure: A) Hazard; B) Vulnerability; C) Exposure; and D) Risk assessment in economic term, derived from their product. In the center of the figure the focus area is indicated by a red star: the hamlet of Patigno, in the municipality of Zeri (northern Tuscany). (For interpretation of the references to colour in this figure legend, the reader is referred to the web version of this article.)

## 6. Discussion

The paper presents a methodological procedure for the assessment of the vulnerability of buildings to slow-moving landslides at the scale of the Northern Apennines. This result is subsequently employed in the context of the application of the QRA technique. In order to assess the components of the risk equation, the methodology exploits open and freely available data at the Italian national scale (i.e., IFFI, TINITALY DEM, OMI), information collected during the surveys carried out in the study areas and it explores the potential of using A-DInSAR Sentinel-1 data to assess the building vulnerability assessment.

The procedure presented has been employed and applied with the objective of advancing the current state of the art in the quantitative vulnerability assessment. In this paper, the authors undertake a rigorous examination of the extant literature to formulate a set of general and specific recommendations for conducting a robust vulnerability analysis through the utilisation of satellite interferometry. As discussed and analysed in the existing scientific literature, the vulnerability assessment represents the most challenging parameter to determine in the risk equation. This is due to the lack of detailed information regarding the buildings, such as the type of construction, the number of floors, the type and depth of the foundations, and, finally, the renovations that may have been carried out. Furthermore, uncertainty exists regarding the relationship between landslide geometry, kinematic, and building response. The topic is explored in considerable detail in the scientific literature, with a variety of approaches being employed. In order to collect comprehensive data on buildings and landslides for integration into the analysis, several approaches were developed at the local scale (Peng et al., 2015). In other instances, in order to overcome the lack of specific information about buildings and landslides, vulnerability assessment relies on data aggregation (Caleca et al., 2022b). Alternatively, in light of the difficulties and uncertainties associated with vulnerability assessment, precautionary approaches adopted it equal to 1 (Uzielli et al., 2008).

The procedure proposed in this paper represents a significant advancement, attempting to overcome the critical limitations of existing methodologies, the constraints related to the scale of the study, the reliance on data aggregation, and the excessive precautionary assumptions. By addressing these challenges, the method ensures a more precise and localized assessment of vulnerability for each structure, setting a new benchmark for accuracy in risk evaluation. This procedure is based on the well-established concepts in the literature regarding the generation of fragility and vulnerability curves (Peduto et al., 2017a) and its unconstrained application, which can be reproduced at different scales of analysis, from local to regional or national levels. The objective of the performed activity was to develop a reproducible and updatable

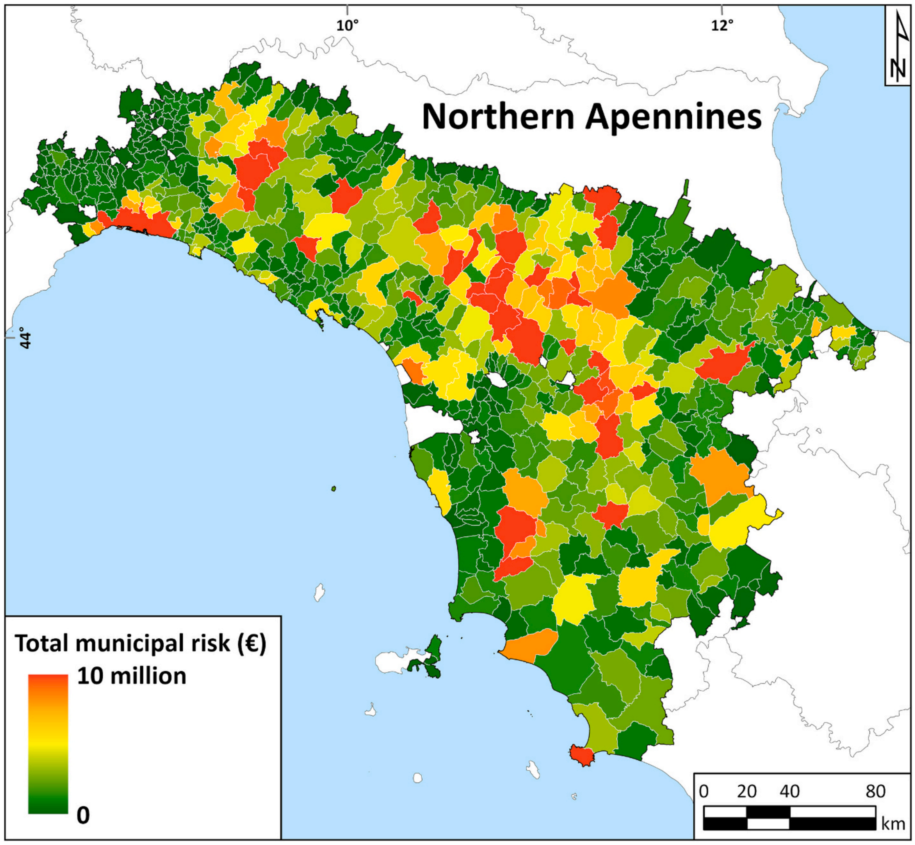


**Fig. 9.** - The total quantitative landslide risk assessment for buildings at the municipal scale in the Northern Apennines.

procedure that, starting from approaches widely consolidated at local scale, could be applied on wide area. It was essential that all the input data used exhibited uniform characteristics at this scale. Consequently, local and municipal datasets, which may provide finer resolution and better granularity of information, were excluded from this analysis as they do not have the necessary coverage. The procedure has been based on the use of comprehensive, standardised, and freely available open cadastral databases, which comprise the essential structural data for the whole Italian territory. The absence of more detailed information has the consequence of a general underestimation of the exposure economic value of buildings, which fails to consider factors such as height and the usage. The capacity to differentiate fundamental parameters of buildings, particularly the type of construction, would improve the generation of fragility and vulnerability curves for each building type. This would enable the delineation of the distinct behaviour exhibited by a masonry building in comparison to a reinforced one.

Another notable advantage of the proposed procedure is represented by the exploitation of the wide spatial and temporal coverage of A-DInSAR data. This is derived from C-band radar images acquired by the Sentinel-1 satellite constellation, allows the quantification of deformation intensity at the regional scale. The 30-m spatial spacing of the vertical and horizontal components derived from C-band Sentinel-1 may represent a potential limitation for detecting narrow landslides, in comparison to the high efficacy demonstrated for large landslides. The utilisation of data with a higher spatial resolution may be a solution to overcome the limitation, but it is important to consider the increase of data volume at the regional or national scales. Consequently, the trade-off between spatial resolution and study scale is a critical factor. The Sentinel-1 imagery represents a valuable resource for the observation of buildings, other anthropogenic structures and vegetated areas, due to their high coherence. Conversely, in dense wooded areas, such as a significant proportion of the Northern Apennines, the coherence rapidly decreases, resulting in the loss of displacement information. The utilisation of L-band radar, distinguished by its 24 cm wavelength, is expected to demonstrate enhanced coherence within vegetated regions and to overcome the limitations encountered with the C-band Sentinel-1. The imminent future will see the advent of freely accessible L-band data, with the launches of two significant missions: the NISAR mission, a joint venture between the National Aeronautics and Space Administration (NASA) and the Indian Space Research Organization (ISRO), and the Copernicus ROSE-L mission by the European Space Agency (ESA). The L-band peculiarities will allow us to overcome the typical limitations of the high frequency systems, operating in C- and X-band, thus improving our monitoring capability in several geohazard scenarios (De Luca et al., 2025). Furthermore, additional constraints imposed by Sentinel-1 SAR technology are associated with both the low sensitivity in the North-South direction due to the near-polar orbit of the satellite and the geometric distortions in mountainous regions, i.e. foreshortening, layover, and shadowing, have an impact on the resulting fragility and vulnerability curves.

A comprehensive validation and comparison with other results available in the literature is challenging due to the differences in scale of analysis and in the approach employed. In the following section, the outcome of this study is compared with the most advanced result for the Italian territory obtained with the methodology proposed by Caleca et al. (2022b). This data set is distinguished by its aggregation into cells measuring 1 km$^2$, encompassing all buildings within the designated area. In order to ensure the reliability of the comparison between the two methodologies, the total building risk is evaluated at the municipality scale.

The comparison between the outcomes of risk in monetary terms is illustrated in Fig. 10A. The two boxplots indicate a considerable discrepancy, up to one order of a magnitude. This is evidenced by the median value of the assessment risk by the proposed procedure being on

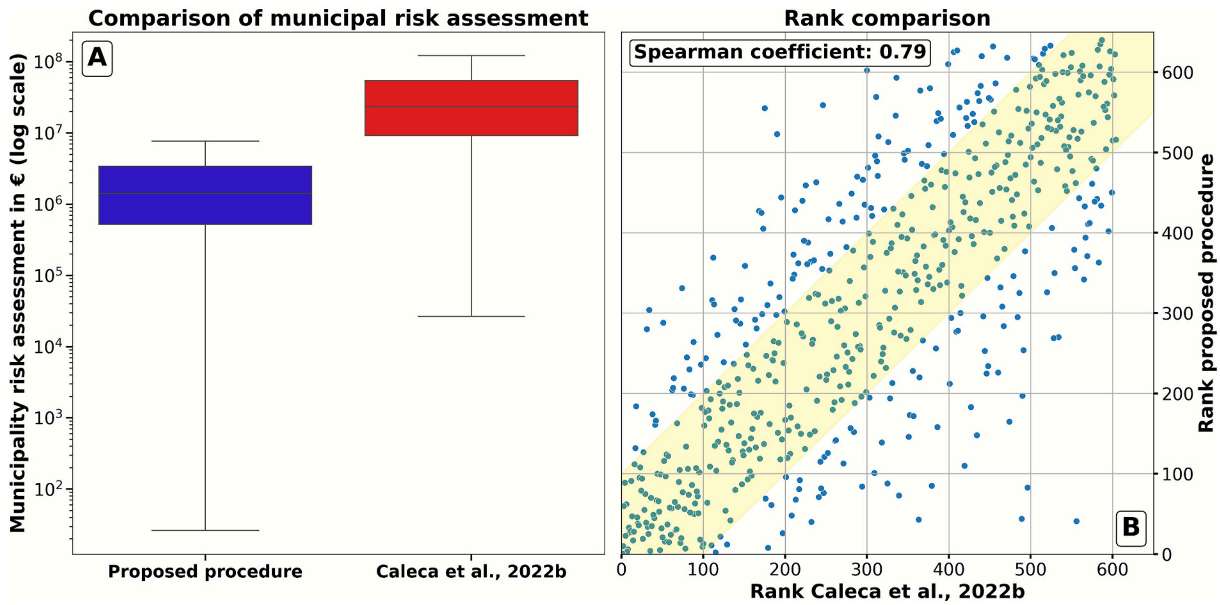


**Fig. 10.** – Comparison of municipal risk assessments between the proposed procedure and the data available in Caleca et al. (2022b). A) The boxplots illustrate the distribution of municipal risk in monetary terms (€). The values are displayed on a logarithmic scale to accentuate the disparities between the two analyses. B) The scatterplot illustrates the comparison between the ranks assigned by the two methods, highlighting the correlation between the rankings for each municipality. The yellow tolerance band indicates the variability between the two methods, suggesting that they are reasonably well-calibrated. (For interpretation of the references to colour in this figure legend, the reader is referred to the web version of this article.)

the order of $10^6$€, while the values reported by Caleca et al. (2022b) are on the order of $10^7$€. As discussed in the contribution of Caleca et al. (2022a), there is a substantial discrepancy between the result of their analysis and the financial resources allocated to risk mitigation measures. Specifically, the authors emphasize an overestimation of risk by one order of magnitude. The primary cause of this discrepancy can be attributed to the utilisation of different scale of resolution. The proposed approach by Caleca et al. (2022b) involves the aggregation of all the data considered into a regular 1 $km^2$ cells, while the data of the financial resources are assessed through a site-specific analysis.

Consequently, the risk assessment performed at the scale of single building in this work may potentially offer a more realistic and commensurate perspective, aligned with the financial resources allocated to risk mitigation measures estimated by Caleca et al. (2022a). It is also noteworthy that the proposed procedure underestimates the total municipal assessment due to the lack of an optimal coverage of A-DInSAR measurements in the vicinity of buildings, which consequently results in the exclusion of a proportion of them from analysis. To ensure a more efficient comparison between the two methodologies, the municipal risk assessments are then ranked (Fig. 10B). The scatterplot illustrates the distribution of the municipalities, with yellow region indicating municipalities that have similar ranks in both methodologies. The evaluation of the comparison is conducted through the utilisation of the Spearman coefficient, which is a measure of rank correlation. The Spearman coefficient ranges from $-1$ (perfect negative correlation) to $+1$ (perfect positive correlation), with values close to 0 indicating no correlation. In this case, the Spearman coefficient of 0.79 suggests a positive correlation between the two methodologies. For instance, in both methodologies the municipality of Genoa, located in the Liguria region, is ranked as first.

The correlation between the degree of damage observed during the surveys and the deformation intensity measured through the A-DInSAR datasets reveals two main limitations. Firstly, the presence of abandoned buildings, categorised within the high damage categories despite their location in a stable area, present difficulties in determining the origin of the fractures and cracks observed on their facades. Secondly, new or restored buildings, exhibiting minimal damage or no cracks in areas of active landslides, present challenges in obtaining information regarding damage before the renovations. In both cases, the primary issue is the absence of the availability of homogenous databases at a national level, and of the documentation pertaining to the history of the building. Nevertheless, a comparison between the quantitative vulnerability assessment yielded by the proposed procedure and the distribution of buildings within or outside the polygons of the IFFI landslide inventory is illustrated in Fig. 11. The analysis indicates that the distribution of buildings within or outside the landslide area varies according to the increasing level of the vulnerability. For the vulnerability values ranging between 0 and 0.2, the majority of buildings are situated outside from landslide polygons. Conversely, as the vulnerability values increased, the percentage of buildings within a landslide polygon became predominant, until at vulnerability values over 0.8, whereby 97 % of buildings are within a landslide. It is notable that no buildings in the Northern Apennines area exhibit vulnerability values exceeding 0.9.

## 7. Conclusion

A methodological procedure for the quantitative building vulnerability assessment triggered by slow-moving landslides is presented. The area of study is the Northern Apennines in central Italy, a region with a high susceptibility to landslides, as evidenced by the IFFI inventory, which reports approximately 200,000 landslides, representing 13.8 % of the surface area.

The proposed procedure is scalable and reproducible, with no constraints on the size of the survey area. It is based on a comprehensive database of information gathered on a specific phenomenon (e.g. slow-moving landslides) and includes parameters related to the intensity of ground deformation and the severity of damage to buildings. The intensity is quantified through the utilisation of freely accessible C-band SAR images acquired by the Sentinel-1 satellite constellation, which have been processed through the P-SBAS DInSAR algorithm. The severity of damage to buildings related to slow-moving landslides has been collected through comprehensive on-site investigations in multiple municipalities across the Northern Apennines, in urban areas with high landslide susceptibility. The field surveys have involved the examination

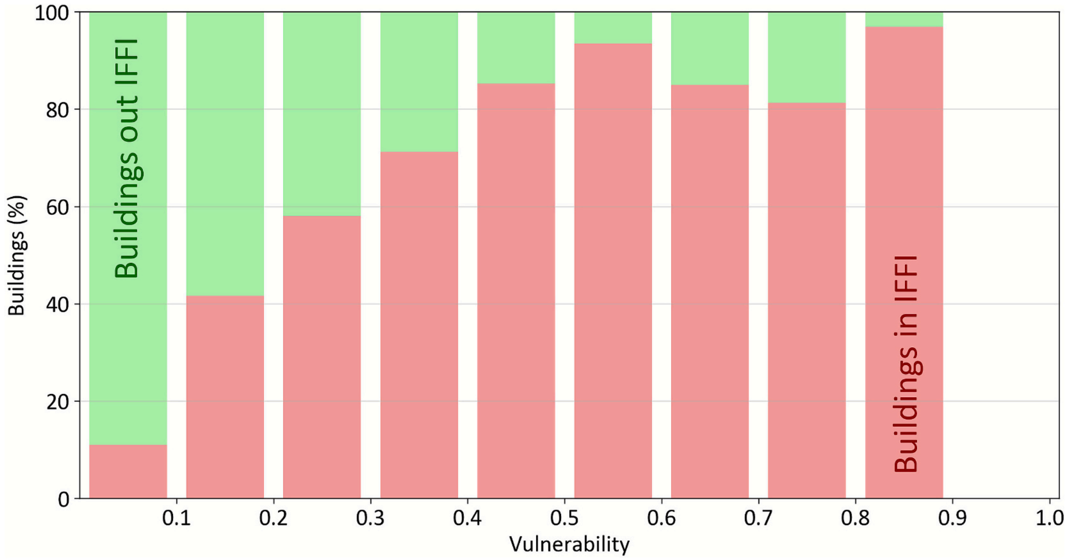


**Fig. 11.** – The chart illustrates the comparison between the quantitative vulnerability assessment values and the distribution of buildings within or outside the polygons of the IFFI inventory. The red-shaded area corresponds to the proportion of buildings located within a landslide polygon as mapped by the IFFI inventory, whereas the green-shaded area indicates buildings situated outside landslide areas. (For interpretation of the references to colour in this figure legend, the reader is referred to the web version of this article.)

of more than 4000 buildings across 18 different municipalities in the regions of Emilia-Romagna, Liguria and Tuscany. These pairs of parameters, i.e. intensity and damage severity, were associated with each building in the Northern Apennines in order to generate the fragility and vulnerability curves, which express the probabilistic relationship between the damage severity of exposed buildings and the landslide intensity. Furthermore, the vulnerability curve is employed within the QRA procedure to define the vulnerability parameter, which is typically the factor that presents the greatest challenge in terms of quantification within the risk equation. A comprehensive evaluation of over 700,000 buildings in the Northern Apennines has been conducted in terms of their landslide risk, encompassing the parameters of hazard, vulnerability, and exposure. The total risk assessed for the building in the Northern Apennines is estimated at approximately 1.8 billion euros. Subsequent analysis involves a comparison of these findings with data from the scientific literature, with particular attention to the results reported in (Caleca et al., 2022b). The analysis reveals a substantial discrepancy in the values of risk assessment, attributable to the different scales of analysis between the two procedures. Specifically, the evaluation by the proposed procedure is an order of magnitude lower. Despite this discrepancy, the proposed approach may offer a more realistic assessment that is better aligned with the financial resources available for risk mitigation. A further exploration of this comparison via rank demonstrates a positive correlation between the two sets of results, as evidenced by a Spearman rank correlation coefficient of 0.79.

The proposed procedure introduces an unprecedented level of wide-scale analysis in the scientific literature, offering an innovative approach to assessing vulnerability and risk. In contradistinction to prior studies, which predominantly concentrate on local scale or aggregated data, this methodology allows for the assessment of the vulnerability of specific structures. Its scope is not confined to evaluating buildings; it can also be used to assess critical infrastructure, such as roads, railways, bridges, and other essential networks. The procedure can be further refined with the ingestion of more detailed information, such as that pertaining to building constructions and foundations. The potential benefits of this approach extend to local administrators involved in urban planning and management. Specifically, it can be used to identify areas most vulnerable to structural damage and optimize the allocation of resources for risk mitigation, including human and financial resources. The capacity to direct targeted interventions, optimize resource allocation, and strengthen territorial resilience represents a paradigm shift in large-scale risk assessment and sets a new benchmark for future studies and disaster management strategies.

## CRediT authorship contribution statement

**Francesco Poggi:** Writing – review & editing, Writing – original draft, Visualization, Validation, Resources, Methodology, Investigation, Formal analysis, Data curation, Conceptualization. **Francesco Caleca:** Writing – review & editing, Validation, Formal analysis. **Olga Nardini:** Investigation. **Francesco Barbadori:** Investigation. **Matteo Del Soldato:** Writing – review & editing, Methodology, Investigation. **Claudio De Luca:** Writing – review & editing, Software, Resources. **Francesco Casu:** Writing – review & editing, Software, Resources. **Manuela Bonano:** Software, Resources. **Riccardo Lanari:** Writing – review & editing, Supervision. **Veronica Tofani:** Writing – review & editing, Supervision. **Federico Raspini:** Writing – review & editing, Supervision.

## Declaration of competing interest

The authors declare no conflict of interest. The funding sponsors had no role in the design of the study; in the collection, analyses, or interpretation of data; in the writing of the manuscript, and in the decision to publish the results.

## Acknowledgements

The SAR image dataset used in the paper for the cases study was provided by the Italian Space Agency (ASI) under the DInSAR-3 M project on “DInSAR Multi-frequenza/Multi-piattaforma per analisi Multi-scala dei movimenti del suolo”. This research was also partially funded by the European Union - NextGeneratonEU (PNRR-M4C2) through the following projects: CN-HPC (CN00000013), CN-MOST (CN00000023), and GeoSciences IR (IR0000037). The present paper was also partially funded by the IREA CNR/ Italian Ministry of Ecologic Transition DGIS 2022-2024 agreement, and it was partially supported by the Italian DPC, in the framework of the IREA-DPC (2022–2024) agreement.

## Appendix A. Appendix

**Table A1**
Dataset of the field surveys conducted in the areas of interest, for each municipality is reported the number of buildings in each classes of severity damage.

| Municipalities | No Damage | Negligible | Weak | Moderate | Severe | Very severe | Potential collapse | Unusable |
|---|---|---|---|---|---|---|---|---|
| Bagnone | 0 | 2 | 39 | 20 | 8 | 6 | 0 | 2 |
| Berceto | 13 | 160 | 57 | 48 | 29 | 9 | 1 | 1 |
| Borzonasca | 0 | 27 | 77 | 41 | 16 | 2 | 7 | 3 |
| Camporgiano | 79 | 114 | 109 | 89 | 16 | 1 | 2 | 0 |
| Cantagallo | 28 | 17 | 17 | 8 | 25 | 6 | 0 | 0 |
| Castelnuovo di Garfagnana | 4 | 24 | 29 | 25 | 11 | 2 | 0 | 0 |
| Chitignano | 31 | 137 | 96 | 76 | 13 | 2 | 0 | 0 |
| Cutigliano | 2 | 17 | 38 | 33 | 25 | 7 | 0 | 0 |
| Ne | 0 | 3 | 15 | 16 | 13 | 15 | 5 | 4 |
| Palanzano | 1 | 3 | 32 | 17 | 3 | 8 | 0 | 0 |
| Pescaglia | 0 | 71 | 57 | 35 | 37 | 3 | 1 | 0 |
| Piazza al Serchio | 10 | 26 | 16 | 23 | 11 | 4 | 0 | 0 |
| Rufina | 0 | 23 | 22 | 15 | 3 | 0 | 0 | 0 |
| Sambuca Pistoiese | 0 | 3 | 17 | 22 | 8 | 3 | 0 | 0 |
| Santo Stefano d'Aveto | 0 | 0 | 26 | 47 | 41 | 54 | 6 | 3 |
| Sillano | 5 | 33 | 26 | 18 | 14 | 0 | 0 | 0 |
| Vaiano | 39 | 63 | 49 | 18 | 0 | 0 | 0 | 0 |
| Zeri | 14 | 571 | 368 | 423 | 134 | 66 | 56 | 36 |

## Data availability

Data will be made available on request.

## References


Antonielli, B., Mazzanti, P., Rocca, A., Bozzano, F., Dei Cas, L., 2019. A-DInSAR performance for updating landslide inventory in mountain areas: an example from Lombardy region (Italy). Geosciences 9, 364. https://doi.org/10.3390/geosciences9090364.

Bamler, R., Hartl, P., 1998. Synthetic aperture radar interferometry. Inverse Probl. 14, R1–R54. https://doi.org/10.1088/0266-5611/14/4/001.

Berardino, P., Fornaro, G., Lanari, R., Sansosti, E., 2002. A new algorithm for surface deformation monitoring based on small baseline differential SAR interferograms. IEEE Trans. Geosci. Remote Sens. 40, 2375–2383. https://doi.org/10.1109/TGRS.2002.803792.

Birkmann, J., 2013. Measuring Vulnerability to Natural Hazards: Towards Disaster Resilient Societies, Measuring Vulnerability to Natural Hazards: Towards Disaster Resilient Societies.

Blaikie, P., Cannon, T., Davis, I., Wisner, B., 2014. At Risk, 0 ed. Routledge. https://doi.org/10.4324/9780203714775.

Breiman, L., 2001. Random forests. Mach. Learn. 45, 5–32. https://doi.org/10.1023/A:1010933404324.

Caleca, F., Tofani, V., Segoni, S., Raspini, F., Franceschini, R., Rosi, A., 2022a. How can landslide risk maps be validated? Potential solutions with open-source databases. Front. Earth Sci. 10, 998885. https://doi.org/10.3389/feart.2022.998885.

Caleca, F., Tofani, V., Segoni, S., Raspini, F., Rosi, A., Natali, M., Catani, F., Casagli, N., 2022b. A methodological approach of QRA for slow-moving landslides at a regional scale. Landslides 19, 1539–1561. https://doi.org/10.1007/s10346-022-01875-x.

Cascini, L., Peduto, D., Pisciotta, G., Arena, L., Ferlisi, S., Fornaro, G., 2013. The combination of DInSAR and facility damage data for the updating of slow-moving landslide inventory maps at medium scale. Nat. Hazards Earth Syst. Sci. 13, 1527–1549. https://doi.org/10.5194/nhess-13-1527-2013.

Castelli, M., Saetta, V., Scavia, C., 2003. Numerical study of scale effects on the stiffness modulus of rock masses. Int. J. Geomech. 3, 160–169. https://doi.org/10.1061/(ASCE)1532-3641(2003)3:2(160).

Casu, F., Elefante, S., Imperatore, P., Zinno, I., Manunta, M., De Luca, C., Lanari, R., 2014. SBAS-DInSAR parallel processing for deformation time-series computation. IEEE J. Sel. Top. Appl. Earth Obs. Remote Sens. 7, 3285–3296. https://doi.org/10.1109/JSTARS.2014.2322671.

Chelli, A., Stefanini, M.C., 1999. Geomorphological features and temporal distribution of the present day landslides activity in the Gordana Basin (Zeri, Northern Apennines): a dendrogeomorphological analysis. In: Geografia Fisica e Dinamica Quaternaria, 9.

Clarivate, A., 2019. Web of Science.

Corominas, J., Van Westen, C., Frattini, P., Cascini, L., Malet, J.-P., Fotopoulou, S., Catani, F., Van Den Eeckhaut, M., Mavrouli, O., Agliardi, F., Pitilakis, K., Winter, M. G., Pastor, M., Ferlisi, S., Tofani, V., Hervás, J., Smith, J.T., 2013. Recommendations for the quantitative analysis of landslide risk. Bull. Eng. Geol. Environ. https://doi.org/10.1007/s10064-013-0538-8.

Crosetto, M., Monserrat, O., Cuevas-González, M., Devanthéry, N., Crippa, B., 2016. Persistent Scatterer interferometry: a review. ISPRS J. Photogramm. Remote Sens. 115, 78–89. https://doi.org/10.1016/j.isprsjprs.2015.10.011.

De Luca, C., Zinno, I., Manunta, M., Lanari, R., Casu, F., 2017. Large areas surface deformation analysis through a cloud computing P-SBAS approach for massive processing of DInSAR time series. Remote Sens. Environ. 202, 3–17. https://doi.org/10.1016/j.rse.2017.05.022.

De Luca, C., Roa, Y.L.B., Bonano, M., Casu, F., Euillades, P., Euillades, L., Franzese, M., Manunta, M., Yasir, M., Onorato, G., Striano, P., Dini, L., Tapete, D., Lanari, R., 2025. SAOCOM-1 L-band DInSAR time series generation through the P-SBAS approach: algorithm extension and products analysis. IEEE J. Sel. Top. Appl. Earth Obs. Remote Sens. 18, 2680–2703. https://doi.org/10.1109/JSTARS.2024.3507554.

Del Soldato, M., Bianchini, S., Calcaterra, D., De Vita, P., Martire, D.D., Tomás, R., Casagli, N., 2017. A new approach for landslide-induced damage assessment. Geomat. Nat. Haz. Risk 8, 1524–1537. https://doi.org/10.1080/19475705.2017.1347896.

Del Soldato, M., Farolfi, G., Rosi, A., Raspini, F., Casagli, N., 2018. Subsidence evolution of the Firenze–Prato–Pistoia plain (Central Italy) combining PSI and GNSS data. Remote Sens. 10, 1146. https://doi.org/10.3390/rs10071146.

Del Soldato, M., Solari, L., Poggi, F., Raspini, F., Tomás, R., Fanti, R., Casagli, N., 2019. Landslide-induced damage probability estimation coupling InSAR and field survey data by fragility curves. Remote Sens. 11, 1486. https://doi.org/10.3390/rs11121486.

Federici, P.R., Alberto, P., Chelli, A., D'Amto, A., Alfredo, G., Ribolini, A., 2001. La grande frana di Patigno di Zeri (Massa-Carrara). MEMORIE DELLA ACCADEMIA LUNIGIANESE DI SCIENZE GIOVANNI CAPELLINI. Scienze Naturali Fisiche e Matematiche 70, 49.

Fell, R., Corominas, J., Bonnard, C., Cascini, L., Leroi, E., Savage, W.Z., 2008. Guidelines for landslide susceptibility, hazard and risk zoning for land use planning. Eng. Geol. 102, 85–98. https://doi.org/10.1016/j.enggeo.2008.03.022.

Ferlisi, S., Peduto, D., Gullà, G., Nicodemo, G., Borrelli, L., Fornaro, G., 2015. The use of DInSAR data for the analysis of building damage induced by slow-moving landslides. In: Lollino, G., Giordan, D., Crosta, G.B., Corominas, J., Azzam, R., Wasowski, J., Sciarra, N. (Eds.), Engineering Geology for Society and Territory- Volume 2. Springer International Publishing, Cham, pp. 1835–1839. https://doi.org/10.1007/978-3-319-09057-3_325.

Ferlisi, S., Nicodemo, G., Peduto, D., 2018. Empirical fragility curves for masonry buildings in slow-moving landslide-affected areas of southern Italy. In: Kallel, A., Ksibi, M., Ben Dhia, H., Khélifi, N. (Eds.), Recent Advances in Environmental Science from the Euro-Mediterranean and Surrounding Regions, Advances in Science. Technology & Innovation. Springer International Publishing, Cham, pp. 1825–1828. https://doi.org/10.1007/978-3-319-70548-4_529.

Ferlisi, S., Gullà, G., Nicodemo, G., Peduto, D., 2019. A multi-scale methodological approach for slow-moving landslide risk mitigation in urban areas, southern Italy. Euro-Mediterr. J. Environ. Integr. 4, 20. https://doi.org/10.1007/s41207-019-0110-4.

Ferlisi, S., Marchese, A., Peduto, D., 2021. Quantitative analysis of the risk to road networks exposed to slow-moving landslides: a case study in the Campania region (southern Italy). Landslides 18, 303–319. https://doi.org/10.1007/s10346-020-01482-8.

Ferretti, A., Prati, C., Rocca, F., 2001. Permanent scatterers in SAR interferometry. IEEE Trans. Geosci. Remote Sens. 39, 8–20. https://doi.org/10.1109/36.898661.

Ferretti, A., Fumagalli, A., Novali, F., Prati, C., Rocca, F., Rucci, A., 2011. A new algorithm for processing interferometric data-stacks: SqueeSAR. IEEE Trans. Geosci. Remote Sens. 49, 3460–3470. https://doi.org/10.1109/TGRS.2011.2124465.

Festa, D., Bonano, M., Casagli, N., Confuorto, P., De Luca, C., Del Soldato, M., Lanari, R., Lu, P., Manunta, M., Manzo, M., Onorato, G., Raspini, F., Zinno, I., Casu, F., 2022.

Nation-wide mapping and classification of ground deformation phenomena through the spatial clustering of P-SBAS InSAR measurements: Italy case study. ISPRS J. Photogramm. Remote Sens. 189, 1–22. https://doi.org/10.1016/j.isprsjprs.2022.04.022.
Fotopoulou, S.D., Pitilakis, K.D., 2013. Fragility curves for reinforced concrete buildings to seismically triggered slow-moving slides. Soil Dyn. Earthq. Eng. 48, 143–161. https://doi.org/10.1016/j.soildyn.2013.01.004.
Fotopoulou, S.D., Pitilakis, K.D., 2017. Probabilistic assessment of the vulnerability of reinforced concrete buildings subjected to earthquake induced landslides. Bull. Earthq. Eng. 15, 5191–5215. https://doi.org/10.1007/s10518-017-0175-x.
Frattini, P., Crosta, G., Allievi, J., 2013. Damage to buildings in large slope rock instabilities monitored with the PSInSAR™ technique. Remote Sens. 5, 4753–4773. https://doi.org/10.3390/rs5104753.
Fuchs, S., Birkmann, J., Glade, T., 2012. Vulnerability assessment in natural hazard and risk analysis: current approaches and future challenges. Nat. Hazards 64, 1969–1975. https://doi.org/10.1007/s11069-012-0352-9.
Giovinazzi, S., Lagomarsino, S., 2004. A Macroseismic Method for the Vulnerability Assessment of Buildings.
Glade, T., 2003. Vulnerability Assessment in Landslide Risk Analysis.
Haklay, M., Weber, P., 2008. OpenStreetMap: user-generated street maps. IEEE Pervasive Comput 7, 12–18. https://doi.org/10.1109/MPRV.2008.80.
Hooper, A., Zebker, H., Segall, P., Kampes, B., 2004. A new method for measuring deformation on volcanoes and other natural terrains using InSAR persistent scatterers. Geophys. Res. Lett. 31. https://doi.org/10.1029/2004GL021737, 2004GL021737.
Hungr, O., Cruden, D., Fell, R., 1997. Some Methods of Landslide Hazard Intensity Mapping, 1st Edition. ed. Landslide Risk Assessment. Routledge.
Iadanza, C., Trigila, A., Starace, P., Dragoni, A., Biondo, T., Roccisano, M., 2021. IdroGEO: a collaborative web mapping application based on REST API services and open data on landslides and floods in Italy. IJGI 10, 89. https://doi.org/10.3390/ijgi10020089.
Lanari, R., Mora, O., Manunta, M., Mallorqui, J.J., Berardino, P., Sansosti, E., 2004. A small-baseline approach for investigating deformations on full-resolution differential SAR interferograms. IEEE Trans. Geosci. Remote Sens. 42, 1377–1386. https://doi.org/10.1109/TGRS.2004.828196.
Luo, H.Y., Zhang, L.M., Zhang, L.L., He, J., Yin, K.S., 2023. Vulnerability of buildings to landslides: the state of the art and future needs. Earth Sci. Rev. 238, 104329. https://doi.org/10.1016/j.earscirev.2023.104329.
Mansour, M.F., Morgenstern, N.R., Martin, C.D., 2011. Expected damage from displacement of slow-moving slides. Landslides 8, 117–131. https://doi.org/10.1007/s10346-010-0227-7.
Manunta, M., De Luca, C., Zinno, I., Casu, F., Manzo, M., Bonano, M., Fusco, A., Pepe, A., Onorato, G., Berardino, P., De Martino, P., Lanari, R., 2019. The parallel SBAS approach for Sentinel-1 interferometric wide swath deformation time-series generation: algorithm description and products quality assessment. IEEE Trans. Geosci. Remote Sens. 57, 6259–6281. https://doi.org/10.1109/TGRS.2019.2904912.
Massonnet, D., Feigl, K.L., 1998. Radar interferometry and its application to changes in the earth's surface. Rev. Geophys. 36, 441–500. https://doi.org/10.1029/97RG03139.
Mavrouli, O., Fotopoulou, S., Pitilakis, K., Zuccaro, G., Corominas, J., Santo, A., Cacace, F., De Gregorio, D., Di Crescenzo, G., Foerster, E., Ulrich, T., 2014. Vulnerability assessment for reinforced concrete buildings exposed to landslides. Bull. Eng. Geol. Environ. https://doi.org/10.1007/s10064-014-0573-0.
Mondini, A.C., Guzzetti, F., Chang, K.-T., Monserrat, O., Martha, T.R., Manconi, A., 2021. Landslide failures detection and mapping using synthetic aperture radar: past, present and future. Earth Sci. Rev. 216, 103574. https://doi.org/10.1016/j.earscirev.2021.103574.
Mora, O., Mallorqui, J.J., Broquetas, A., 2003. Linear and nonlinear terrain deformation maps from a reduced set of interferometric Sar images. IEEE Trans. Geosci. Remote Sens. 41, 2243–2253. https://doi.org/10.1109/TGRS.2003.814657.
Negulescu, C., Foerster, E., 2010. Parametric studies and quantitative assessment of the vulnerability of a RC frame building exposed to differential settlements. Nat. Hazards Earth Syst. Sci. 10, 1781–1792. https://doi.org/10.5194/nhess-10-1781-2010.
Nicodemo, G., Peduto, D., Ferlisi, S., Maccabiani, J., 2016. Investigating building settlements via very high resolution SAR sensors. In: Life-Cycle of Engineering Systems: Emphasis on Sustainable Civil Infrastructure. CRC Press, p. 8.
Norris, M., Oppenheim, C., 2007. Comparing alternatives to the web of science for coverage of the social sciences' literature. J. Inf. Secur. 1, 161–169. https://doi.org/10.1016/j.joi.2006.12.001.
Novellino, A., Cesarano, M., Cappelletti, P., Di Martire, D., Di Napoli, M., Ramondini, M., Sowter, A., Calcaterra, D., 2021. Slow-moving landslide risk assessment combining machine learning and InSAR techniques. CATENA 203, 105317. https://doi.org/10.1016/j.catena.2021.105317.
Onorato, G., De Luca, C., Casu, F., Manunta, M., Yasir, M., Noli, P., Striano, P., Lanari, R., 2025. Identification and correction of phase unwrapping errors in multi-temporal small baseline DInSAR interferograms: a three-step cascade algorithm. IEEE J. Sel. Top. Appl. Earth Obs. Remote Sens. 1–16. https://doi.org/10.1109/JSTARS.2025.3546824.
Osmanoğlu, B., Dixon, T.H., Wdowinski, S., Cabral-Cano, E., Jiang, Y., 2011. Mexico City subsidence observed with persistent scatterer InSAR. Int. J. Appl. Earth Obs. Geoinf. 13, 1–12. https://doi.org/10.1016/j.jag.2010.05.009.
Parisi, F., Sabella, G., 2017. Flow-type landslide fragility of reinforced concrete framed buildings. Eng. Struct. 131, 28–43. https://doi.org/10.1016/j.engstruct.2016.10.013.
Peduto, D., Ferlisi, S., Nicodemo, G., Reale, D., Pisciotta, G., Gullà, G., 2017a. Empirical fragility and vulnerability curves for buildings exposed to slow-moving landslides at medium and large scales. Landslides 14, 1993–2007. https://doi.org/10.1007/s10346-017-0826-7.
Peduto, D., Nicodemo, G., Maccabiani, J., Ferlisi, S., 2017b. Multi-scale analysis of settlement-induced building damage using damage surveys and DInSAR data: a case study in the Netherlands. Eng. Geol. 218, 117–133. https://doi.org/10.1016/j.enggeo.2016.12.018.
Peng, L., Xu, S., Hou, J., Peng, J., 2015. Quantitative risk analysis for landslides: the case of the three gorges area, China. Landslides 12, 943–960. https://doi.org/10.1007/s10346-014-0518-5.
Pepe, A., Lanari, R., 2006. On the extension of the minimum cost flow algorithm for phase unwrapping of multitemporal differential SAR Interferograms. IEEE Trans. Geosci. Remote Sens. 44, 2374–2383. https://doi.org/10.1109/TGRS.2006.873207.
Raspini, F., Bianchini, S., Ciampalini, A., Del Soldato, M., Montalti, R., Solari, L., Tofani, V., Casagli, N., 2019. Persistent Scatterers continuous streaming for landslide monitoring and mapping: the case of the Tuscany region (Italy). Landslides 16, 2033–2044. https://doi.org/10.1007/s10346-019-01249-w.
Raspini, F., Caleca, F., Del Soldato, M., Festa, D., Confuorto, P., Bianchini, S., 2022. Review of satellite radar interferometry for subsidence analysis. Earth Sci. Rev. 235, 104239. https://doi.org/10.1016/j.earscirev.2022.104239.
Rosi, A., Tofani, V., Tanteri, L., Tacconi Stefanelli, C., Agostini, A., Catani, F., Casagli, N., 2018. The new landslide inventory of Tuscany (Italy) updated with PS-InSAR: geomorphological features and landslide distribution. Landslides 15, 5–19. https://doi.org/10.1007/s10346-017-0861-4.
Saygili, G., Rathje, E.M., 2009. Probabilistically based seismic landslide hazard maps: an application in Southern California. Eng. Geol. 109, 183–194. https://doi.org/10.1016/j.enggeo.2009.08.004.
Segoni, S., Battistini, A., Rossi, G., Rosi, A., Lagomarsino, D., Catani, F., Moretti, S., Casagli, N., 2014. Technical Note: An Operational Landslide Early Warning System at Regional Scale Based on Space–Time Variable Rainfall Thresholds. https://doi.org/10.5194/nhessd-2-6599-2014.
Solari, L., Del Soldato, M., Bianchini, S., Ciampalini, A., Ezquerro, P., Montalti, R., Raspini, F., Moretti, S., 2018. From ERS 1/2 to Sentinel-1: subsidence monitoring in Italy in the last two Decades. Front. Earth Sci. 6, 149. https://doi.org/10.3389/feart.2018.00149.
Tarquini, S., Nannipieri, L., 2017. The 10 m-resolution TINITALY DEM as a trans-disciplinary basis for the analysis of the Italian territory: current trends and new perspectives. Geomorphology 281, 108–115. https://doi.org/10.1016/j.geomorph.2016.12.022.
Tomás, R., Pagán, J.I., Navarro, J.A., Cano, M., Pastor, J.L., Riquelme, A., Cuevas-González, M., Crosetto, M., Barra, A., Monserrat, O., Lopez-Sanchez, J.M., Ramón, A., Ivorra, S., Del Soldato, M., Solari, L., Bianchini, S., Raspini, F., Novali, F., Ferretti, A., Costantini, M., Trillo, F., Herrera, G., Casagli, N., 2019. Semi-automatic identification and pre-screening of geological–geotechnical deformational processes using persistent Scatterer interferometry Datasets. Remote Sens. 11, 1675. https://doi.org/10.3390/rs11141675.
Torres, R., Snoeij, P., Geudtner, D., Bibby, D., Davidson, M., Attema, E., Potin, P., Rommen, B., Floury, N., Brown, M., Traver, I.N., Deghaye, P., Duesmann, B., Rosich, B., Miranda, N., Bruno, C., L'Abbate, M., Croci, R., Pietropaolo, A., Huchler, M., Rostan, F., 2012. GMES Sentinel-1 mission. Remote Sens. Environ. 120, 9–24. https://doi.org/10.1016/j.rse.2011.05.028.
Trigila, A., Iadanza, C., Spizzichino, D., 2010. Quality assessment of the Italian landslide inventory using GIS processing. Landslides 7, 455–470. https://doi.org/10.1007/s10346-010-0213-0.
Trigila, A., Frattini, P., Casagli, N., Catani, F., Crosta, G., Esposito, C., Iadanza, C., Lagomarsino, D., Mugnozza, G.S., Segoni, S., Spizzichino, D., Tofani, V., Lari, S., 2013. Landslide susceptibility mapping at National Scale: The Italian case study. In: Margottini, C., Canuti, P., Sassa, K. (Eds.), Landslide Science and Practice. Springer, Berlin Heidelberg, Berlin, Heidelberg, pp. 287–295. https://doi.org/10.1007/978-3-642-31325-7_38.
Uzielli, M., Nadim, F., Lacasse, S., Kaynia, A.M., 2008. A conceptual framework for quantitative estimation of physical vulnerability to landslides. Eng. Geol. 102, 251–256. https://doi.org/10.1016/j.enggeo.2008.03.011.